

12

TN NO: N-1710

TITLE: A STUDY OF COUPLING THE BOUNDARY AND FINITE ELEMENT METHODS IN TWO-DIMENSIONAL ELASTOSTATICS

AUTHOR: T. A. Shugar and J. V. Cox

DATE: October 1984

SPONSOR: Naval Material Command

PROGRAM NO: ZR000-001-179

NOTE

NAVAL CIVIL ENGINEERING LABORATORY
PORT HUENEME, CALIFORNIA 93043

Approved for public release; distribution unlimited.

DTIC
ELECTIC
S JAN 29 1985 D
A

85 01 22 012

AD-A149 619

DTIC FILE COPY

TECHNICAL

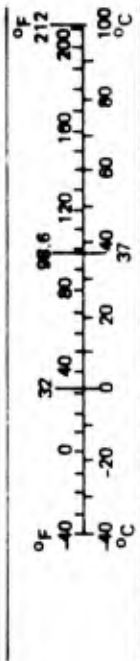
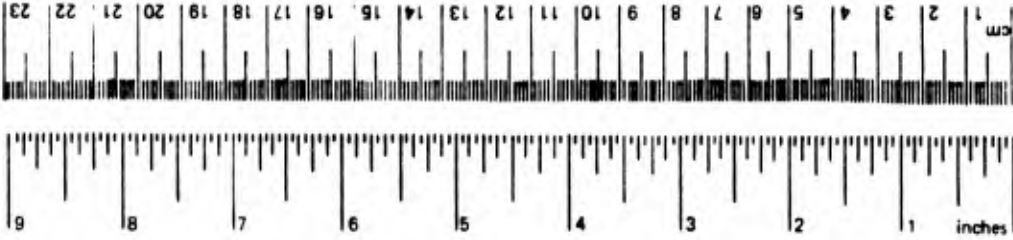
METRIC CONVERSION FACTORS

Approximate Conversions to Metric Measures

Symbol	When You Know	Multiply by	To Find	Symbol
		LENGTH		
in	inches	* 2.5	centimeters	cm
ft	feet	30	centimeters	cm
yd	yards	0.9	meters	m
mi	miles	1.6	kilometers	km
		AREA		
in ²	square inches	6.5	square centimeters	cm ²
ft ²	square feet	0.09	square meters	m ²
yd ²	square yards	0.8	square meters	m ²
mi ²	square miles	2.6	square kilometers	km ²
	acres	0.4	hectares	ha
		MASS (weight)		
oz	ounces	28	grams	g
lb	pounds	0.45	kilograms	kg
	short tons	0.9	tonnes	t
	(2,000 lb)			
		VOLUME		
tsp	teaspoons	5	milliliters	ml
Tbsp	tablespoons	15	milliliters	ml
fl oz	fluid ounces	30	milliliters	ml
c	cups	0.24	liters	l
pt	pints	0.47	liters	l
qt	quarts	0.95	liters	l
gal	gallons	3.8	liters	l
ft ³	cubic feet	0.03	cubic meters	m ³
yd ³	cubic yards	0.76	cubic meters	m ³
		TEMPERATURE (exact)		
°F	Fahrenheit temperature	5/9 (after subtracting 32)	Celsius temperature	°C

Approximate Conversions from Metric Measures

When You Know	Multiply by	To Find	Symbol
	LENGTH		
millimeters	0.04	inches	in
centimeters	0.4	inches	in
meters	3.3	feet	ft
kilometers	1.1	yards	yd
	0.6	miles	mi
	AREA		
square centimeters	0.16	square inches	in ²
square meters	1.2	square yards	yd ²
square kilometers	0.4	square miles	mi ²
hectares (10,000 m ²)	2.5	acres	
	MASS (weight)		
grams	0.035	ounces	oz
kilograms	2.2	pounds	lb
tonnes (1,000 kg)	1.1	short tons	
	VOLUME		
milliliters	0.03	fluid ounces	fl oz
liters	2.1	pints	pt
liters	1.06	quarts	qt
liters	0.26	gallons	gal
cubic meters	35	cubic feet	ft ³
cubic meters	1.3	cubic yards	yd ³
	TEMPERATURE (exact)		
Celsius temperature	9/5 (then add 32)	Fahrenheit temperature	°F



*1 in = 2.54 (exact). For other exact conversions and more detailed tables, see NBS Misc. Publ. 286, Units of Weights and Measures, Price \$2.25, SD Catalog No. C13 10 286.

Unclassified

SECURITY CLASSIFICATION OF THIS PAGE (When Data Entered)

REPORT DOCUMENTATION PAGE		READ INSTRUCTIONS BEFORE COMPLETING FORM
1 REPORT NUMBER TN-1710	2 GOVT ACCESSION NO. DN187255	3 RECIPIENT'S CATALOG NUMBER
4 TITLE (and Subtitle) A STUDY OF COUPLING THE BOUNDARY AND FINITE ELEMENT METHODS IN TWO- DIMENSIONAL ELASTOSTATICS		5 TYPE OF REPORT & PERIOD COVERED No. final; Oct 1982 - Sep 1983
		6 PERFORMING ORG. REPORT NUMBER
7 AUTHOR(s) T. A. Shugar and J. V. Cox		8 CONTRACT OR GRANT NUMBER(s)
9 PERFORMING ORGANIZATION NAME AND ADDRESS NAVAL CIVIL ENGINEERING LABORATORY Port Hueneme, California 93043		10 PROGRAM ELEMENT, PROJECT, TASK AREA & WORK UNIT NUMBERS 61152N; ZR000-001-179
11 CONTROLLING OFFICE NAME AND ADDRESS Naval Material Command Washington, DC 20360		12 REPORT DATE October 1984
		13 NUMBER OF PAGES 65
14 MONITORING AGENCY NAME & ADDRESS (if different from Controlling Office)		15 SECURITY CLASS (of this report) Unclassified
		15a DECLASSIFICATION/DOWNGRADING SCHEDULE
16 DISTRIBUTION STATEMENT (of this Report) Approved for public release; distribution unlimited.		
17 DISTRIBUTION STATEMENT (of the abstract entered in Block 20, if different from Report)		
18 SUPPLEMENTARY NOTES		
19 KEY WORDS (Continue on reverse side if necessary and identify by block number) Boundary element, finite element, elastostatics, coupling, microcomputers		
20 ABSTRACT (Continue on reverse side if necessary and identify by block number) This report investigates the potential advantage of a combined boundary element-finite element solution approach by examining the behavior of coupled elastostatic domains. A theoretical investigation of coupling the displacement-based finite element method with the indirect boundary element method was conducted and the results were implemented within a microcomputer framework. It is believed that a combined finite element and boundary element computer program could reduce the high cost now associated with nonlinear finite		

continued

DD FORM 1 JAN 73 1473 EDITION OF 1 NOV 65 IS OBSOLETE

Unclassified

SECURITY CLASSIFICATION OF THIS PAGE (When Data Entered)

Unclassified

SECURITY CLASSIFICATION OF THIS PAGE(When Data Entered)

20. Continued

element programs, but it is shown that further work is needed to make the boundary element method more effective. A quadratic, isoparametric boundary element, which would allow a better evaluation of accuracy and cost in the solution of coupled elastostatic problems, should be investigated.

Library Card

Naval Civil Engineering Laboratory
A STUDY OF COUPLING THE BOUNDARY AND FINITE
ELEMENT METHODS IN TWO-DIMENSIONAL ELASTOSTATICS,
by T. A. Shugar and J. V. Cox

TN-1710 65 pp illus October 1984 Unclassified

1. Elastostatics 2. Microcomputers 1. ZR000-001-179

This report investigates the potential advantage of a combined boundary element-finite element solution approach by examining the behavior of coupled elastostatic domains. A theoretical investigation of coupling the displacement-based finite element method with the indirect boundary element method was conducted and the results were implemented within a microcomputer framework. It is believed that a combined finite element and boundary element computer program could reduce the high cost now associated with nonlinear finite element programs, but it is shown that further work is needed to make the boundary element method more effective. A quadratic, isoparametric boundary element, which would allow a better evaluation of accuracy and cost in the solution of coupled elastostatic problems, should be investigated.

*Additional keywords: numerical analysis,
integral equations*

Unclassified

SECURITY CLASSIFICATION OF THIS PAGE(When Data Entered)

CONTENTS

	Page
INTRODUCTION	1
Objective	1
Background	2
Scope	3
COUPLING THEORY	4
Two-Dimensional Elastostatics Boundary Value Problem	7
The Finite Element Method in Ω^1	8
The Indirect Boundary Element Method in Ω^2	14
Coupling the Finite Element and Indirect Boundary Element Equations	18
EXPERIMENTAL NUMERICAL IMPLEMENTATION	19
SOME NUMERICAL RESULTS	24
Axially Loaded Plane Stress Model	25
Cavity in an Infinite Medium	27
SUMMARY	28
CONCLUSIONS	29
RECOMMENDATIONS	30
REFERENCES	31
APPENDIXES	
A - Boundaries and Boundary Conditions in the Finite Element Modeling of Soils	A-1
B - Aspects of the Finite Element Implementation	B-1
C - Coupling Algorithm	C-1



Distribution For	
DTIC GRA&I	<input checked="" type="checkbox"/>
DTIC TAB	<input type="checkbox"/>
Unannounced	<input type="checkbox"/>
Justification	
Distribution/	
Availability Codes	
Dist	Avail and/or Special
A1	

INTRODUCTION

In nonlinear finite element problems, particularly continuum problems, much of the problem is, in fact, linear and homogeneous in its behavior. Further, these characteristics can often be recognized by the analyst at the outset. These facts have motivated research towards the development of general-purpose nonlinear computer programs that possess a combined solution concept that treats the linear, homogeneous part of the problem with the boundary integral equation formulation and the nonlinear part with the finite element (FE) formulation.

The boundary integral equation method or its numerical implementation, the boundary element (BE) method, has only recently been given much attention as a general solution scheme for linear, homogeneous boundary value problems. It is a solution strategy for such problems in its own right, but here it competes with the more universal finite element methods or finite difference methods. However, the latter methods are more suited to the solution of nonlinear problems as well. Today it is well accepted among researchers that nonlinear continuum problems are too costly, and as a result most research today is directed at making nonlinear analyses more affordable. Thus, a primary contribution of the boundary integral equation methods may well turn out to be reduction in the costs of nonlinear analyses.

In this report the potential of a combined solution approach is investigated by examining the behavior of the coupled domains.

Objective

The ultimate objective of this research is to determine whether or not the boundary element and finite element solution methods can be combined with advantage towards more economical solutions of nonlinear

structural problems. The immediate emphasis will be on the interface conditions and the methodology necessary to combine the solution methods and the resulting behavior of the implementation.

Background

About 12 years ago, as today, the analysis of geotechnical structures in a semi-infinite medium with finite element methods was very common. The problem of the influence of artificial boundaries at finite distances from the structure was recognized more or less as a necessary evil in the modeling procedure, as there was no practical alternative to the specification of these boundary conditions.

To minimize the problem, a systematic convergence study was conducted. An unpublished, actual case study illustrating this method is included in Appendix A. Several successive computer runs, each with a corresponding increase in the geometrical extent surrounding the structure, were made, while the response of most interest was observed. The procedure was continued until this response seemed to converge within some tolerance that was satisfactory to the analyst. The necessary increase in the size of the finite element model caused the cost of each analysis to successively increase. Because of the uncertainty in the final size necessary for satisfactory accuracy, planning the resources necessary for accomplishing the analysis was difficult. This difficulty is severely compounded in a nonlinear finite element framework.

The technique that held the most promise of resolving the difficulty at that time was the global-local finite element method, which was developed originally by Mote (1971). This, so far, has not proven to be the case. Two other (newer) methods now seem to be more promising. These are the method of using infinite finite elements, first developed by Bettess (1977), and the method of using a combined boundary/domain solution, which is to be studied in this investigation.

The first examples of using a combined solution approach were Chen and Mei (1974) and Shaw (1974). Neither study was concerned with a semi-infinite soil medium, but instead they dealt with wave phenomena in media that possessed both a homogeneous and an inhomogeneous region.

The former region was treated with a boundary solution method and the latter region with a domain method. A theoretical study, of a distinctly mathematical nature, of the combined solution approach was conducted by Atluri and Grannell (1978). Many applications of combined solution methods have occurred (e.g., water wave problems by Zienkiewicz et al. (1977), electromagnetic field problems by Lean et al. (1979), acoustic field problems by Shaw (1979), and geotechnical problems). The so-called coupled-field problems, such as in Fellipa et al. (1974), wherein the differential operators are different in adjacent domains, are omitted from the perspective of this study, although these, too, are sometimes approached by combined solution methods.

The research that came closest to the direction that is pursued in this report is the works by Beer and Meek (1981) and Beer (1983a and b). Here comparisons are given for the numerical performance of boundary elements and infinite elements in geotechnical applications.

Other studies on the mechanics of coupling approximation theories include Fellipa et al. (1974), Shaw and Falby (1978), Shaw (1978), Zienkiewicz et al. (1978), Kelly et al. (1979), Mustoe (1979), and Brebbia and Georgiou (1979).

Scope

This study was carried out in a microcomputer framework. The numerical demonstration problems are correspondingly small. But since the focus of the study is upon the interface between the boundary element and finite element regions, small problems do not pose an inconvenience.

The programs used in the study are written in Pascal. Pascal is a modern programming language in which programs are comparatively more easy to debug and maintain in a microcomputer environment as contrasted with FORTRAN. Further, modularity is supported well, particularly in UCSD Pascal, through the use of library units. Modularity is deemed very important by Fellipa (1981) relative to coupled field software applications. The authors believe this to be true also of research software dealing with coupled solution methods of any type.

Combined boundary and finite element solutions are applied to small two-dimensional elastostatic problems. The indirect boundary element method (BEM) is used as the boundary solution method and the displacement-based finite element method (FEM) as the domain method. Simple element formulations are used in both cases. The indirect boundary element program is a Pascal-conversion of a FORTRAN program developed earlier that used constant elements (Shugar and Cox, 1983). The finite element and coupling programs were written during the present investigation. The finite element program uses the constant strain triangle element.

Coupling of the BE and FE methods can take two approaches. The first approach views the boundary element region as a super finite element (Zienkiewicz et al., 1977; and Kelly et al., 1979), in which case the BE equations are developed in a symmetric manner. This is an efficient method if a relatively small BE system is being coupled with a large FE system. The main advantage of this method of coupling is that the resulting algebraic system of equations that must be solved is symmetric. Existing methods for the efficient solution of sparse, symmetric systems can then be used.

As the relative size of the BE system increases, the greater effort of developing the symmetric BEM equations outweighs the reduced effort of solving a symmetric system of equations. At this point the second approach is more efficient. This approach views the FE region as a homogeneous BE region (Brebbia, 1978). The BE system of equations is nonsymmetric.

COUPLING THEORY

The general problem that is to be solved numerically by some approximation theory is stated in the conventional boundary value problem form in the following. The nonlinear partial differential equation,

$$L_N \phi = \bar{f} \quad \text{in } \Omega$$

where L_N is a nonlinear operator, ϕ is the unknown function sought, and \bar{f} is the prescribed data (force, temperature, etc.). This equation is presumed to govern throughout the domain Ω , shown in Figure 1. Further, on the boundary Γ of the domain there are, in general, two boundary conditions to be satisfied,

$$A \phi = \bar{g} \quad \text{on } \Gamma^A$$

$$B \phi = \bar{h} \quad \text{on } \Gamma^B$$

where A and B are likewise differential operators but presumed here to be linear, and \bar{g} and \bar{h} are prescribed data on the boundary.

While the nonlinear equation suffices to govern throughout Ω , there is a portion of Ω where the behavior of the solution is linear. Therefore, the domain is divided into two subdomains: Ω^1 , in which the behavior is nonlinear; and Ω^2 , in which the behavior is linear. The subdomains share a common boundary as shown in Figure 2.

By way of an example nonlinear equation, the nonlinear operator may be defined as

$$L_N = \frac{\partial}{\partial t} - \left(\frac{\partial}{\partial x} \right)^2 - \phi \left(\frac{\partial^2}{\partial x^2} \right)$$

and the data $\bar{f} = 0$. This equation describes the one-dimensional, nonlinear unsaturated flow through porous media, where $\phi(x,t)$ is the water table height, for example, during drawdown of a reservoir adjacent to the confining porous medium (Bruch and Zyvoloski, 1973).

One way to solve the nonlinear problem is to first linearize it. (Another way is to apply explicit finite difference to it, as is.) This method begins by introducing an initial guessed solution, ϕ_g , such that the differential equation is linearized. The linear operator in this case would be

$$L = \frac{\partial}{\partial t} - \frac{\partial \phi_g}{\partial x} \frac{\partial}{\partial x} - \phi_g \frac{\partial^2}{\partial x^2}$$

where with $\bar{f} = 0$, the linearized differential equation is

$$L \phi = 0 \quad \text{in } \Omega$$

The boundary conditions are not important in this example and are therefore omitted. This equation is thereafter solved by some standard numerical, approximation theory. The result ϕ is compared to ϕ_g , and if the comparison is satisfactory, convergence has been achieved, and ϕ is the solution sought. Otherwise ϕ_g is systematically changed (for example, replaced by the latest value of ϕ) and the solution procedure is repeated. The iterative process continues until convergence is achieved. Depending on the strength of the nonlinear terms, many iterations of the above scheme may be required to achieve convergence.

So long as the solution in Ω^2 can be assumed to behave linearly, the solution for the entire domain Ω is more efficiently obtained if the iterative nonlinear solution scheme is confined to Ω^1 , while a linear solution procedure is used in Ω^2 . However, in general, this is not standard procedure, and a nonlinear finite element (or finite difference) solution procedure is used throughout Ω . Thus, an unnecessarily large problem is solved during the nonlinear, iterative solution process. This inefficiency is further compounded when, as is most often the case in practice, multiple analyses of the problem are conducted.

What is required is a combined solution procedure for such problems in which the two subdomains, Ω^1 and Ω^2 , can be defined a priori. For example, many geotechnical problems involving semi-infinite media fall into this class. The exact demarcation between the linear and nonlinear subdomains does not need to be known in advance, for the location of the boundary can always be prescribed in a conservative fashion while still retaining the prospect of substantial savings in cost of analysis.

Nothing said so far relates to the appropriate numerical, approximation theories to be applied to the two subdomains, Ω^1 and Ω^2 . In fact, it would seem possible to retain the prospect of the savings just stated while using the same approximation theory in both regions. However, in this study, the finite element method shall be used in Ω^1 and the boundary element method shall be used in Ω^2 .

Since the amount of benefit to be derived from a combined solution approach depends on the number of nonlinear solution iterations required for convergence in Ω^1 , as well as on other problem-dependent characteristics, quantification of these benefits will not be emphasized in this study for the sake of brevity. Instead, the mechanics of coupling the two approximation theories mentioned above will be emphasized. And further, for that purpose, only a linear differential equation operator in the subdomain Ω^1 will be used for clarity and simplicity of presentation. Extension to a nonlinear problem should be straightforward in principle, only more lengthy from an implementation standpoint.

Two-Dimensional Elastostatics Boundary Value Problem

The class of problems to which the combined solution method is applied in this study is illustrated in Figure 3 and is described as follows: Find the stress components σ_{ij} and the displacement components u_i that satisfy the following governing equations of equilibrium (body forces are assumed to be zero):

$$\left. \begin{aligned} \frac{\partial \sigma_{xx}}{\partial x} + \frac{\partial \sigma_{xy}}{\partial y} &= 0 \\ \frac{\partial \sigma_{yy}}{\partial y} + \frac{\partial \sigma_{xy}}{\partial x} &= 0 \end{aligned} \right\} \text{ in } \Omega \quad (1)$$

and the boundary conditions,

$$u_i = \bar{u}_i \quad \text{on } \Gamma^A \quad (2)$$

$$\sigma_{ij} n_j = \bar{t}_i \quad \text{on } \Gamma^B \quad (3)$$

where \bar{u}_i and \bar{t}_i are prescribed displacements along the boundary Γ^A and prescribed tractions along the boundary segment Γ^B , respectively, and n_j is the direction cosines for a point on Γ^B .

This class of problems will be solved numerically and will use the finite element method to one side of the artificial boundary Γ^{12} and the indirect boundary element method to the other side.

The Finite Element Method in Ω^1

As shown in Figure 4, the domain Ω has been divided into two subdomains, Ω^1 and Ω^2 . Here the solution in Ω^1 is described using the finite element method. The elastostatics boundary value problem will be confined, for the moment, to only Ω^1 , and its solution is to proceed independently of Ω^2 . Thus, the governing equations apply as stated above except that the domains are changed to Ω^1 in the region and Γ^{A1} and Γ^{B1} on the boundaries. In addition, to account for conditions on the new boundary Γ^{12} , a displacement compatibility equation is written as

$$u_i - u_i^b = 0 \quad \text{on } \Gamma^{12} \quad (4)$$

where $u_i^b = u(x^+)$. The point x^+ approaches indefinitely the point $x \in \Gamma^{12}$ from the right in Figure 4. This interface condition specifies the continuity of displacement across the artificial boundary. Though u_i^b is unknown, it is convenient to think of it as a prescribed quantity until later when the boundary element solution procedure is addressed in Ω^2 .

The derivation of the finite element solution procedure is conveniently approached in this case by the principle of minimum potential energy because this approach easily incorporates the needed constraint equations on the artificial boundary into the finite element formulation (see Gallagher (1975) for example).

The potential energy Π for the subdomain Ω^1 is written as

$$\Pi = \int_{\Omega^1} \frac{1}{2} (\sigma_{xx} \epsilon_{xx} + \sigma_{yy} \epsilon_{yy} + 2 \sigma_{xy} \epsilon_{xy}) d\Omega - \int_{\Gamma^{B1}} (\bar{t}_x u + \bar{t}_y v) d\Gamma$$

where the strain tensor components ϵ_{ij} are defined as

$$\epsilon_{ij} = \frac{1}{2} \left(\frac{\partial u_i}{\partial x_j} + \frac{\partial u_j}{\partial x_i} \right)$$

It is assumed that $\bar{u}_i = 0$, so that no potential energy is contributed by the reaction forces along Γ^{A1} . However, the energy of the interface condition must be included since u_i^b is, in general, nonzero. This is accomplished by augmenting the potential energy with the product of the given constraint equation and Lagrange multiplier components, λ_i . The augmented potential energy is written as

$$\Pi^a = \Pi + \int_{\Gamma^{12}} (u_i - u_i^b) \lambda_i d\Gamma$$

The Lagrange multiplier components are additional unknowns in the energy description. It will be especially important later to recognize them as traction components along Γ^{12} . This can be seen here since the integral on Γ^{12} must have units of energy for consistency. The Lagrange multipliers are further interpreted as the tractions necessary to maintain displacement compatibility along the artificial boundary.

The augmented potential energy can now be subdivided as follows:

$$\Pi^a = \sum_{e=1}^{NE} \Pi_e^a$$

where NE is the number of subdivisions of the subdomain Ω^1 . That is, in set notation,

$$\Omega^1 \approx \left\{ \Omega_e^1 \mid e = 1, 2, \dots, NE \right\}$$

Since this subdivision may not have smooth edges along the boundary Γ^1 , it is recognized as an approximation. The augmented potential energy for each subdivision is

$$\begin{aligned} \Pi_e^a &= \int_{\Omega_e^1} \frac{1}{2} (\sigma_{xx} \varepsilon_{xx} + \sigma_{yy} \varepsilon_{yy} + 2 \sigma_{xy} \varepsilon_{xy}) d\Omega \\ &\quad - \int_{\Gamma_e^{B1}} \bar{t}_i u_i d\Gamma + \int_{\Gamma_e^{12}} (u_i - u_i^b) \lambda_i d\Gamma \end{aligned}$$

For convenience, this expression can be written in matrix form. To do this, the following one-dimensional matrices are first defined:

$$\begin{aligned} \underline{\underline{\sigma}}' &= \begin{bmatrix} \sigma_{xx} & \sigma_{yy} & \sigma_{xy} \end{bmatrix} \\ \underline{\underline{\varepsilon}}' &= \begin{bmatrix} \varepsilon_{xx} & \varepsilon_{yy} & \gamma_{xy} \end{bmatrix} \quad \text{where } \gamma_{xy} = 2 \varepsilon_{xy} \\ \underline{\underline{u}}' &= [u, v] \\ \underline{\underline{\bar{t}}}' &= \begin{bmatrix} \bar{t}_x & \bar{t}_y \end{bmatrix} \\ \underline{\underline{\lambda}}' &= \begin{bmatrix} \lambda_x & \lambda_y \end{bmatrix} \end{aligned}$$

The superscript prime denotes the matrix transpose. Further, let the linear, elastic stress-strain relations represent plane strain conditions as follows:

$$\underline{\underline{\sigma}} = \underline{\underline{D}} \underline{\underline{\varepsilon}}$$

$$\text{where } \underline{D} = \frac{E}{1 - \nu^2} \begin{bmatrix} 1 & \nu & 0 \\ \nu & 1 & 0 \\ 0 & 0 & \frac{1-\nu}{2} \end{bmatrix}$$

and where E is Young's modulus and ν is Poisson's ratio for the material comprising the subdomain Ω^1 .

After substituting the above matrices into the total energy expression and the stress-strain relations into the strain energy expression, the following matrix form is obtained for the augmented potential energy of a typical subdivision, e :

$$\Pi_e^a = \frac{1}{2} \int_{\Omega_e^1} \underline{\varepsilon}' \underline{D} \underline{\varepsilon} d\Omega - \int_{\Gamma_e^{B1}} \underline{\bar{t}}' \underline{u} d\Gamma + \int_{\Gamma_e^{12}} (\underline{u} - \underline{u}^b)' \underline{\lambda} d\Gamma$$

Next, it is assumed that Ω_e^1 is a triangular-shaped subdomain as shown in Figure 5. The displacement components u and v are approximated by interpolating them linearly within the triangle as follows:

$$u \approx \sum_{i=1}^3 N_i u_i$$

$$v \approx \sum_{i=1}^3 N_i v_i$$

where N_i is the well-known finite element constant strain triangle (CST) polynomial shape functions. The discrete internal nodal point displacement components at the corner i are, from here on, u_i and v_i .

Further, for the present, interpolate the unknown displacements u_i^b along Γ^{12} in the same way for consistency. Thus,

$$u^b \approx \sum_{i=1}^3 N_i u_i^b$$

$$v^b \approx \sum_{i=1}^3 N_i v_i^b$$

The prescribed tractions \bar{t}_i are often interpolated as statically equivalent constant tractions between the nodes along the boundary Γ^{B1} in finite element analysis. The Lagrange multipliers can also be interpolated as constants along Γ^{12} in the same way. Thus,

$$\int_{\Gamma_e} \bar{t}' \cdot \underline{u} \, d\Gamma \approx \bar{t}_{xe} \sum_{i=1}^3 u_i \int_{\Gamma_e} N_i \, d\Gamma + \bar{t}_{ye} \sum_{i=1}^3 v_i \int_{\Gamma_e} N_i \, d\Gamma$$

$$\int_{\Gamma_e} (\underline{u} - \underline{u}^b)' \cdot \underline{\lambda} \, d\Gamma \approx \lambda_{xe} \sum_{i=1}^3 (u_i - u_i^b) \int_{\Gamma_e} N_i \, d\Gamma \\ + \lambda_{ye} \sum_{i=1}^3 (v_i - v_i^b) \int_{\Gamma_e} N_i \, d\Gamma$$

When the various interpolation schemes are substituted into the augmented potential energy matrix expression, the scalar Π_e^a becomes a function of the discrete nodal variables as follows:

$$\Pi_e^a = \Pi_e^a(u_i, v_i, \lambda_{xe}, \lambda_{ye})$$

The principle of minimum potential energy is used to find the conditions under which the unknown discrete variables can be found. These conditions are (see Gallagher, 1975):

$$\frac{\partial \Pi_e^a}{\partial u_i} = 0, \quad \frac{\partial \Pi_e^a}{\partial v_i} = 0, \quad (i = 1, 2, 3)$$

and

$$\frac{\partial \pi_e^a}{\partial \lambda_{xe}} = 0, \quad \frac{\partial \pi_e^a}{\partial \lambda_{ye}} = 0$$

When the first two partial derivatives are evaluated for an element, the resulting equations are the discrete system of linear algebraic equations representing equilibrium for that finite element in a local coordinate system. When the equations for all finite elements are transformed from the local to the global reference system and then assembled, they can be written as

$$\underline{\underline{K}} \underline{\underline{D}} + \underline{\underline{E}} \underline{\underline{\Lambda}} = \underline{\underline{Q}} \quad (5)$$

These are equations of equilibrium expressed in terms of unknown external nodal point displacement vector $\underline{\underline{D}}$, unknown external element traction vector along the interface $\underline{\underline{\Lambda}}$, and known external nodal point force vector $\underline{\underline{Q}}$, which is formed from the prescribed tractions.* The global stiffness matrix is $\underline{\underline{K}}$, and the coefficient matrix $\underline{\underline{E}}$ contains entries formed by integrating the shape functions N_i along the interface boundary Γ^{12} .

When the last two partial derivative conditions are evaluated and then expressed in terms of global variables, the result can be written as

$$\underline{\underline{D}}^f - \underline{\underline{D}}^b = \underline{\underline{0}} \quad (6)$$

*The vector $\underline{\underline{D}}$ henceforth is used for displacements and is not to be confused with the elasticity matrix. Further, "external displacements" means the same as "global displacements."

This is the prescribed displacement constraint equation on the artificial interface boundary expressed in terms of external nodal displacements on the boundary Γ^{12} . The vector \underline{D}^f is composed of those entries in \underline{D} that correspond to nodes on Γ^{12} . The vector \underline{D}^b represents global displacements for the same nodes, but they are determined by the boundary element solution in Ω^2 .

The Indirect Boundary Element Method in Ω^2

Here the governing equations of elastostatics and the boundary conditions, Equations 1 to 3, are applied to the subdomain Ω^2 and its boundary Γ^2 , respectively, as shown in Figure 6. Thus, to the boundary conditions on Γ^{A2} and Γ^{B2} , a displacement compatibility condition at the artificial boundary Γ^{12} is appended to complete the formulation of the problem independently of the left side of Ω . This condition is

$$u_i - u_i^f = 0 \quad \text{on } \Gamma^{12} \quad (7)$$

where $u_i^f = u_i(x^-)$, and the point x^- approaches indefinitely the point $x \in \Gamma^{12}$ from the left side. Here u_i^f is treated as if it were known.

The indirect boundary integral equations appropriate to this problem can be found in Banerjee and Butterfield (1981). For the subdomain Ω^2 these equations are as follows. For displacements of a point x^0 on the boundaries Γ^{A2} and Γ^{12} ,

$$\bar{u}_i(x^0) = \int_{\Gamma^2 \cup \Gamma^{12}} G_{ij}(x^0, \xi) P_j(\xi) d\Gamma + C_i, \quad (x^0 \in \Gamma^{A2})$$

$$u_i^f(x^0) = \int_{\Gamma^2 \cup \Gamma^{12}} G_{ij}(x^0, \xi) P_j(\xi) d\Gamma + C_i, \quad (x^0 \in \Gamma^{12})$$

and for tractions of a point x^0 on the boundaries Γ^{B2} and Γ^{12} ,

$$\bar{t}_i(x^0) = \frac{1}{2} \delta_{ik} P_k(x^0) + \text{pr.v.} \int_{\Gamma^2 \cup \Gamma^{12}} F_{ik}(x^0, \xi) P_k(\xi) d\Gamma, \quad (x^0 \in \Gamma^{B2})$$

$$t_i(x^0) = \frac{1}{2} \delta_{ik} P_k(x^0) + \text{pr.v.} \int_{\Gamma^2 \cup \Gamma^{12}} F_{ik}(x^0, \xi) P_k(\xi) d\Gamma, \quad (x^0 \in \Gamma^{12})$$

The point x^0 must have a unique tangent, otherwise the constant is other than 1/2 in the last two equations.

The fundamental singular solutions G_{ij} and F_{ik} , which are also known as infinite-space Green's functions, are the heart of the boundary integral method. They are classical results from the theory of elasticity, and for plane strain conditions are given by the following formulas:

$$G_{ij}(x, \xi) = C_1 \left(C_2 \delta_{ij} \ln r - \frac{y_i y_j}{r^2} \right) + A_{ij}$$

$$F_{ij}(x, \xi) = \frac{C_3}{r_3} \left[C_4 (n_k y_i - n_i y_k) + \left(C_4 \delta_{ik} + \frac{2 y_i y_k}{r^2} \right) y_j n_j \right]$$

where $C_1 = \frac{1}{8 \pi \mu (1 - \nu)}$

$$C_2 = 3 - 4 \nu$$

$$C_3 = \frac{1}{4 \pi (1 - \nu)}$$

$$C_4 = 1 - 2 \nu$$

$$y_i = x_i - \xi_i, \quad y_j = x_j - \xi_j, \quad y_k = x_k - \xi_k$$

$$r^2 = y_\ell y_\ell$$

$$\delta_{ij} = \begin{cases} 1 & i = j \\ 0 & i \neq j \end{cases}$$

The term A_{ij} is a constant tensor that is chosen to make G_{ij} zero at some arbitrary distance from the load point. The quantities μ and ν are the shear modulus and Poisson ratio for the material in Ω^2 , respectively.

When $x = \xi$, the function $\ln r$ is weakly singular as shown in Figure 7a, and the function $1/r$ is strongly singular as shown in Figure 7b. Integrals involving weakly singular functions will always exist in the normal sense of integration even when $x = \xi$. However, integrals involving strongly singular terms must be interpreted in the Cauchy principal value sense (i.e., in the sense of a limiting value as $x \rightarrow \xi$).

$P_j(\xi)$ is the only term normally presumed unknown in the above indirect boundary integral equations. This term represents an artificial distribution of tractions around the entire boundary, $\Gamma^2 \cup \Gamma^{12}$, of Ω^2 . The point ξ is a member of the set of points constituting this boundary, $\xi \in (\Gamma^2 \cup \Gamma^{12})$.

In the strategy of the indirect boundary element method, once the artificial tractions are solved, the stresses and displacements for any point in the subdomain Ω^2 or on its boundary are found by formulas that are similar to those above for u_i and t_i . These formulas are not presented here for the sake of brevity. Thus, the artificial tractions $P_j(\xi)$ play the same, unknown-variable role in the indirect boundary element method as the displacements $u_i(x,y)$ in the displacement-based finite element method.

The indirect boundary element procedure is the process of integrating numerically the above indirect boundary integral equations. The boundaries Γ^2 and Γ^{12} are subdivided into N_2 and M straight line segments, respectively, for a total of $S_2 = N_2 + M$ segments entirely enclosing Ω^2 . The source density function $P_j(\xi)$ is approximated by interpolation in terms of discrete nodal values P_{je} associated with each segment e . These segments may be called boundary elements since the discretization and interpolation are similar to the finite element method.

The discretized boundary integral equations, or boundary element equations, for a point x^ℓ at the center of a typical element are:

$$\bar{u}_i(x^\ell) \quad \bar{D}_{i\ell} = \sum_{e=1}^{S_2} \left[P_{je} \int_{\Gamma_e} G_{ij}(x^\ell, \xi) d\Gamma + C_{ie} \right], \quad (x^\ell \in \Gamma^{A2})$$

$$u_i^f(x^l) \quad D_{i\ell}^f = \sum_{e=1}^{S2} P_{je} \int_{\Gamma_e} G_{ij}(x^l, \xi) d\Gamma + C_{ie} \quad , \quad (x^l \in \Gamma^{12})$$

$$\bar{t}_i(x^l) \quad \bar{T}_{i\ell} = \frac{1}{2} \delta_{ik} P_k(x^l) + \sum_{e=1}^{S2} P_{ke} \int_{\Gamma_e} F_{ik}(x^l, \xi) d\Gamma \quad ,$$

. (x^l ∈ Γ^{B2})

$$t_i(x^l) \quad T_{i\ell} = \frac{1}{2} \delta_{ik} P_k(x^l) + \sum_{e=1}^{S2} P_{ke} \int_{\Gamma_e} F_{ik}(x^l, \xi) d\Gamma \quad ,$$

. (x^l ∈ Γ¹²)

In the above equations, the external (global) displacements are $D_{i\ell}$ and the external tractions are $T_{i\ell}$. The superscript bar, as usual, indicates that the value is prescribed.

After the indicated integrations over the length of each boundary element are carried out, a coupled set of four systems of linear algebraic equations in the unknown artificial traction vector \underline{P} may be formed. The set of equations may be expressed as

$$\underline{G}^{A2} \underline{P} = \underline{\bar{D}} \quad (8)$$

$$\underline{G}^{12} \underline{P} = \underline{D}^f \quad (9)$$

$$\underline{F}^{B2} \underline{P} = \underline{\bar{T}} \quad (10)$$

$$\underline{F}^{12} \underline{P} = \underline{T} \quad (11)$$

In what follows, these equations are combined and coupled with the discrete finite element equations, Equations 5 and 6, developed earlier.

Coupling the Finite Element and Indirect Boundary Element Equations

The boundary value problem in the domain Ω , as expressed by Equations 1, 2, and 3, was discretized by two different numerical processes. The finite element method was used in the subdomain Ω^1 and resulted in the algebraic system of Equations 5 and 6. The indirect boundary element method was used in the complementary subdomain Ω^2 and resulted in the linear algebraic system represented by Equations 8 through 11.

An accounting of the entries in the unknown vectors \underline{D} , $\underline{\Lambda}$, \underline{D}^D , \underline{T} , and \underline{P} reveals that the number of unknowns exceeds by $2M$ (M is the number of nodes along Γ^{12}) the number of equations available for solution, Equations 5, 6, and 8 through 11. Apparently another interface condition besides the displacement compatibility condition of Equation 6 is required to obtain a solvable system.

The additional interface condition is provided by equilibrium consideration as follows. The vector $\underline{\Lambda}$ represents the discrete tractions that act on Ω^1 along Γ^{12} . These tractions must be in equilibrium with those that act on Ω^2 along Γ^{12} and that are represented by the vector \underline{T} . Thus, the required $2M$ additional equation is:

$$\underline{\Lambda} + \underline{T} = \underline{0} \quad (12)$$

The unknown vector $\underline{\Lambda}$ can be eliminated from the total system by combining Equations 11 and 12 and substituting the result for $\underline{\Lambda}$ in Equation 5. The result is

$$\underline{K} \underline{D} - \underline{E} \underline{F}^{12} \underline{P} = \underline{\bar{Q}} \quad (13)$$

To eliminate \underline{D}^f from the total system, it is first necessary to partition Equation 13 as follows:

$$\left[\begin{array}{c|c} \underline{K}_{11} & \underline{K}_{12} \\ \hline \underline{K}_{21} & \underline{K}_{22} \end{array} \right] \begin{Bmatrix} \underline{D}^i \\ \underline{D}^f \end{Bmatrix} - \begin{Bmatrix} \underline{0} \\ \underline{E} \underline{F}^{12} \underline{P} \end{Bmatrix} = \begin{Bmatrix} \underline{\bar{Q}} \\ \underline{0} \end{Bmatrix} \quad (13a)$$

where the vector \underline{D}' is simply constituted of all the elements of \underline{D} exclusive of those in \underline{D}^f . Upon substituting the left-hand side of Equation 9 for \underline{D}^f , the partitioned system becomes,

$$\left[\begin{array}{c|c} \underline{K}_{11} & (\underline{K}_{12} \underline{G}^{12}) \\ \hline \underline{K}_{21} & (\underline{K}_{22} \underline{G}^{12}) \end{array} \right] \begin{pmatrix} \underline{D}' \\ \underline{P} \end{pmatrix} - \begin{pmatrix} \underline{Q} \\ \underline{E} \underline{F}^{12} \underline{P} \end{pmatrix} = \begin{pmatrix} \underline{Q} \\ \underline{Q} \end{pmatrix} \quad (13b)$$

Thus, the displacement vector \underline{D}^f is eliminated.

Combining Equation 13b with Equations 8 and 9, the total system in final, reduced form is represented by the following linear algebraic system of equations:

$$\left[\begin{array}{c|c} \underline{K}_{11} & (\underline{K}_{12} \underline{G}^{12}) \\ \hline \underline{K}_{21} & (\underline{K}_{22} \underline{G}^{12} - \underline{E} \underline{F}^{12}) \\ \hline \underline{Q} & \underline{G}^{A2} \\ \hline \underline{Q} & \underline{F}^{B2} \end{array} \right] \begin{pmatrix} \underline{D}' \\ \underline{P} \end{pmatrix} = \begin{pmatrix} \underline{Q} \\ \underline{Q} \\ \underline{D} \\ \underline{T} \end{pmatrix} \quad (14)$$

Once Equation 14 is solved for \underline{D}' and \underline{P} , the displacements \underline{D}^f can be found from Equation 9. Then \underline{D} is entirely known and the finite element stresses in Ω^1 can be calculated in the usual way. And with \underline{P} known, the displacements and stresses for any specified point in Ω^2 , or on its boundary, can also be calculated in the usual way for the indirect boundary element method.

EXPERIMENTAL NUMERICAL IMPLEMENTATION

The theory for the coupling of finite element and boundary element equations was presented in the previous section. The purpose of this section is to present some implementation aspects of this coupling theory.

All programs are implemented in the Pascal language on an Apple microcomputer. The boundary element method (BEM) program is a Pascal version of the FORTRAN program presented in a previous report (Shugar and Cox, 1983). The finite element method (FEM) program and the coupling programs were written during the course of this study. Some aspects of the FEM program are discussed in Appendix B. At this time, all of the programs are at a research-and-development stage.

The coupling of the FEM and BEM takes the point of view that well-tested finite element and boundary element codes already exist. The existing codes are best viewed as a group of modules each with a distinct task. From an implementation viewpoint, both the FEM and BEM can be broken into three tasks:

1. Develop the system of equations
2. Solve the system of equations
3. Calculate internal responses

In the FEM the system of equations is a result of discretizing the domain into elements, then expressing the displacement field in terms of nodal displacements. These unknown nodal displacements are related to the applied nodal forces in Equation 5. When Lagrange multipliers are not involved it is expressed as

$$\underline{K} \underline{D} = \underline{Q} \quad (15)$$

where \underline{K} , \underline{D} , and \underline{Q} represent the structural stiffness matrix, unknown external nodal displacements, and applied external nodal loads, respectively. Solution of the system of equations yields the external nodal displacements. From these nodal displacements internal responses, such as stresses and strains, can be calculated.

In the indirect BEM the system of equations is a result of discretizing the boundary of the domain into elements, then expressing the known boundary values in terms of artificial boundary tractions. The distribution of the unknown artificial boundary tractions is expressed

in terms of discrete nodal values and is related to the known boundary values in Equations 8 through 11. Combining the equations for an uncoupled BE domain, the system is expressed as

$$\underline{FG} \underline{P} = \underline{KBV} \quad (16)$$

where \underline{FG} is the system matrix, \underline{P} is the nodal artificial boundary tractions, and \underline{KBV} is the vector of known boundary values of displacements and tractions.

With an overview of the system of equations that results from each method, the logistics of the coupling can be further considered. A modular approach to the coupling, as outlined above, requires minimal modification of the individual programs. A schematic of the program interaction is shown in Figure 8. The intent in the modular design is to allow the alternative of both of the codes to be used as stand-alone or coupled stress analysis tools. The dashed lines represent the steps of the schematic for uncoupled analyses. This software strategy is reminiscent of the "partitioned solution" approach suggested by Fellipa (1981) for dynamic problems.

Development of the system of equations requires minimal modification of the existing codes. As explained in the previous section, the nonsymmetric coupling requires compatibility and equilibrium to be satisfied explicitly. Thus, for the interface nodes the BEM code must generate equations for known boundary tractions and displacements. This requires modification of the existing BEM code only if it is limited to homogeneous problems (i.e., if it consists of only one bounded region). However, this modification does not otherwise place any restrictions on the stand-alone BEM code. The BEM and FEM codes begin by reading their respective input data files and end by writing their equations to secondary storage.

The additional step of coupling the two systems of equations is the focus of this study. The coupling and solution steps become part of the same program for this implementation. The program begins with the coupling routine reading a file, which provides for the connectivity

between the BEM and FEM regions. Then the BEM and FEM systems are read and inserted into the combined system. Details of the coupling algorithm are presented in Appendix C. With the equations coupled the solution routine can be brought into memory by overlaying and then used to solve the system of equations. In this study a Gauss elimination procedure with scaled partial pivoting is used to solve the system of equations in which a full matrix is assumed. (Iterative techniques for linear systems may also be used.) Once the system is solved the nodal displacements and artificial tractions are written to the appropriate files on secondary storage.

The files created by the coupling solution program are identical to those created by the stand-alone BEM and FEM codes. Thus, the programs representing the third step in the analysis, calculation of the internal responses, require no modification.

This study is restricted to the coupling of multiple FEM regions to only one BEM region. Nonetheless, one BEM region is adequate for many practical problems, and insight toward more efficient algorithms can be gained. To explain the algorithm used in the coupling, the coupled system of equations must be considered. The systems of equations for both the BEM and FEM were presented in Equations 15 and 16.

Coupling the BEM and FEM systems requires involving equilibrium at the interface. The matrix $\underline{\underline{E}}$, introduced in Equation 5, was formed by integrating the shape functions N_i along the interface boundary Γ^{12} . In this particular implementation an incompatible interface is used, where the displacements along the edge of the finite element vary linearly and those along the boundary element are constant. With this incompatibility $\underline{\underline{E}}$ must be developed in a different manner. From an intuitive approach $\underline{\underline{E}}$ can be shown to be a diagonal matrix of the interface element lengths (times -1). Consider equilibrium at a nodal point along the interface. The BEM considers the boundary tractions as continuous stresses rather than discrete nodal forces. For a constant distribution boundary element, each row of Equation 11 multiplied by the length of the interface element converts the traction to a nodal force. This is mathematically equivalent to multiplying $\underline{\underline{E}}$ by $\underline{\underline{F}}^{12}$, where $\underline{\underline{E}}$ is the diagonal matrix of interface

element lengths (times -1). Assuming no loads on the interface nodes, the interface equations can be extracted from Equation 13 and can be rewritten as

$$\underline{\underline{E}} \underline{\underline{F}}^{12} \underline{\underline{P}} - (\underline{\underline{K}}_{21} \mid \underline{\underline{K}}_{22}) \underline{\underline{D}} = \underline{\underline{0}} \quad (17)$$

where: $\underline{\underline{E}}$ = diagonal matrix of interface element negative lengths
 $\underline{\underline{F}}^{12}$ = coefficient matrix from Equation 11
 $\underline{\underline{P}}$ = vector of unknown artificial boundary tractions
 $(\underline{\underline{K}}_{21} \mid \underline{\underline{K}}_{22})$ = portion of the structure stiffness matrix that relates displacements to forces at the interface nodes
 $\underline{\underline{D}}$ = vector of external nodal displacements

For a homogeneous BEM code, where there is no provision for the interface of two regions, the multiplication of $\underline{\underline{E}}$ and $\underline{\underline{F}}^{12}$ is most readily performed when developing the BEM equations. For a more general nonhomogeneous code, converting the tractions to nodal values when coupling the equations might be more efficient. The first approach was taken in this study.

The second condition to be satisfied at the interface is compatibility. This condition was expressed in Equation 6 as

$$\underline{\underline{D}}^f - \underline{\underline{D}}^b = \underline{\underline{0}}$$

where $\underline{\underline{D}}^f$ and $\underline{\underline{D}}^b$ are the interface node displacements obtained from the finite and boundary element methods, respectively. Equation 6 can be rewritten in terms of the system unknowns by expressing the boundary element displacements in terms of the artificial boundary tractions and using an array $\underline{\underline{A}}$ to extract the interface displacements from the total FEM displacement vector. The compatibility equation is now given by

$$(\underline{\underline{0}} \mid -\underline{\underline{A}}) \underline{\underline{D}} + \underline{\underline{G}}^{12} \underline{\underline{P}} = \underline{\underline{0}} \quad (18)$$

where \underline{A} is a rectangular matrix with columns composed of identity vectors, \underline{D} is the finite element displacement vector, and $\underline{G}^{12} \underline{P}$ is taken from Equation 9.

The coupled system of equations is obtained by combining Equations 15 through 18. Equations 15 and 16 must be satisfied in the FEM and BEM domains, respectively, while Equations 17 and 18 impose equilibrium and compatibility conditions, respectively, at the interface. The coupled system of equations can be written as

$$\begin{bmatrix} \underline{FG}^1 & \underline{0} & \underline{0} \\ \underline{G}^{12} & \underline{0} & -\underline{A} \\ -\underline{E} \underline{F}^{12} & \underline{K}_{12} & \underline{K}_{22} \\ \underline{0} & \underline{K}_{11} & \underline{K}_{12} \end{bmatrix} \begin{Bmatrix} \underline{P} \\ \underline{D}' \\ \underline{D}^f \end{Bmatrix} = \begin{Bmatrix} \underline{KBV} \\ \underline{0} \\ \underline{0} \\ \underline{Q} \end{Bmatrix} \quad (19)$$

Figure 9 graphically represents the nonzero entries in the coefficient matrix of Equation 19 for the problem shown in Figure 10. A one-to-one correspondence exists between the submatrices shown in this figure and those of the above coefficient matrix. The sparsity of the finite element equations is clearly exhibited and contrasts sharply with the density of the boundary element equation.

This system can be reduced to the system of Equation 14 by eliminating the interface displacements, \underline{D}^f , from the vector of unknowns. However, the full system of equations presented in Equation 19 is better suited for implementation since the system of equations is partitioned.

SOME NUMERICAL RESULTS

Two problems are presented in this study of the behavior of the coupled solution technique. The first problem, an axially loaded plane stress model, involves a rectangular membrane. The restraints are applied to the boundary element region and the loads are applied to the finite element region. The second problem is a plane strain problem

consisting of a lined, cylindrical tunnel surrounded by an infinite medium. The liner is modeled by finite elements and the infinite medium by boundary elements. The elements in both methods are relatively crude; thus, the accuracy is of secondary interest. The behavior at the interface is of primary interest. The amount of computational time for each domain of the analysis is also presented in the first problem.

Axially Loaded Plane Stress Model

The model for this problem is shown in Figure 10. The right edge of the boundary element region, elements 10 to 14, is fixed.

The solution times for each major step of the combined analysis are presented in Table 1. The operation steps, except the solution of the system of equations, required considerable disk input/output (I/O) operations. It is instructive to look at the execution times in a relative manner since they are strongly dependent upon the type of device used for secondary storage. (In this study a hard disk was used to store all data files. This is the fastest type of secondary storage device available for a microcomputer with the exception of disk emulators.) As mentioned in the EXPERIMENTAL NUMERICAL IMPLEMENTATION section, a full matrix solution routine was used to solve the system of equations. The solution step could be made faster with a routine that avoids operations on zero entries of the matrix.

The listed execution times indicate that the BEM is considerably slower. It differs by almost a factor of 2 in the formation of the equation and by slightly more than a factor of 5 in the calculation of an equivalently sized field response. In practical BEM analysis, however, large homogeneous domains are subdivided into smaller domains to reduce the solution time. Execution times shown for the two methods, however, do not indicate the total cost of the analysis since they exclude the analyst's labor cost in the development of the model. The labor cost is expected to be greater for the FEM since more prescribed data are required.

Table 2 gives the axial stress values for each of the finite elements above the axis of symmetry (Figure 10). The corresponding boundary element values are recorded for points that are symmetrically located

about the interface from the finite element centers. The restrained end of the boundary element region introduces a Poisson effect; the stress values should all approach unity with distance from this end.

The primary interest is in the percent difference in the finite element and boundary element stresses as the interface is traversed. The data for elements 25 to 28 show that the difference is affected by the proximity of the upper plate boundary. If the interface is traversed there, the percent difference is greater (7%) than if it is traversed along the symmetry axis (1%). The accuracy of the boundary element stress is more adversely affected by the upper plate boundary.

In examining the error of the BEM region one must consider that for the indirect method the BEM region can exactly represent a constant stress field only in the limit as the size of the elements approaches zero. Conversely, the CST finite element (except for numerical inaccuracies) can exactly represent the constant stress field.

The displaced structure is indicated in Figure 11. Arrows are used in the BEM region to indicate the displacements of sample response points.

Figure 12 shows the interface displacements. Because of the constant distribution boundary elements used, a stair-stepping effect occurs near the restrained corner of the BEM region. As mentioned in the EXPERIMENTAL NUMERICAL IMPLEMENTATION section, this coupling has involved incompatible edge displacements at the interface. Compatibility is satisfied at the nodes, however. In this problem smaller boundary elements are placed near the free edge of the plate along the interface. This modeling scheme compensates for the center node of the boundary element not coinciding with the outside node of the corner element. Though these two nodes do not coincide, they have been coupled through the compatibility equations so that they have the same displacements. The smaller displacements of boundary elements 1 and 5 reduce the displacements of finite element nodes 25 and 21, respectively. This contributes to the increased stress in finite elements 32 and 25 (see Table 2).

Cavity in an Infinite Medium

This problem represents a cavity subjected to an internal pressure (100 psi) in an infinite medium. The models for this problem are shown in Figures 13 and 14 (one-quarter of the domain is illustrated). It is modeled as a plane strain problem where the FEM region could possibly represent a pipe or tunnel liner. Both regions are of the same material for easy comparison with elasticity theory. The ability of the BEM region to accurately model the infinite domain relates directly to its potential application in soil-structure interaction problems and geotechnical problems.

Two models are used in this coupled problem. Each uses a different technique for the interface between the FEM and BEM regions. The first model, Figure 13, contains alternative gaps and overlaps with none of the coupled interface nodes coinciding. The second model, Figure 14, adjusts the position of the interface nodes so that the corresponding coupled boundary element and finite element nodes actually coincide, but at the expense of creating a larger gap. Radial stress results for the two models as a function of distance from the cavity center are presented in Table 3. Included also are values from elasticity theory and the results from both direct and indirect BEM solutions incorporating constant elements.

Results for coupled model 1 are presented in Figure 15. The highest radial stress value plotted is the computed finite element stress in the cavity liner. This value should not exceed 100. This inaccuracy in the FEM region is somewhat expected; a constant strain element is used in the region of maximum gradient. The important result of this coupled problem is the demonstrated ability of the computed stress gradient to transcend the interface in a relatively continuous manner.

Coupled model 1 is comparable in accuracy to the 12-element indirect BEM model, both of which are more accurate than model 2, which includes the large gaps. Thus, in this case, forcing nodes to coincide along the interface did not pay dividends.

The direct BEM results (Brebbia, 1978) are the most accurate at the distances considered. However, as the response points in the surrounding medium near the boundary elements, the strong singularity in the direct method can be expected to cause the response to blow up as discussed in Banerjee and Butterfield (1981). This behavior is not shown here because the nearest response point is still too distant to capture that inaccuracy. The 24-element indirect BEM model gives results slightly less accurate than the direct BEM model, but would be expected to behave better near the cavity surface. This is one reason why the indirect method appears preferable (Shugar and Cox, 1983).

Considering the coarseness of the model and the inaccuracy of the elements used, this problem illustrated reasonably well the ability of computed stress gradients to pass through the interface region in a continuous manner. The accuracy was acceptable in the BEM region. For a soil-structure interaction problem where boundary elements are used to model the infinite medium, the constant distribution boundary element might prove to be sufficiently accurate. For problems where accuracy near the interface is required, a higher order boundary element would be needed.

SUMMARY

A theoretical investigation of coupling the displacement-based finite element method with the indirect boundary element method was conducted and the results were implemented within a microcomputer framework. The class of engineering problems that was addressed was limited to two-dimensional elastostatics. The study emphasized the interface conditions between the subdomains in which the two techniques were applied and the behavior of the computed response across that interface.

Prior to coupling the finite element and boundary element methods, a simple finite element computer program was written in Pascal, and a previously written boundary element computer program was converted from FORTRAN to Pascal.

The coupling method used was based on direct satisfaction of displacement compatibility and force equilibrium conditions at node points along the common border between the two subdomains. Lagrange multipliers, which introduce the necessary constraint equations imposed by the above conditions, were used to facilitate the mathematical description of the coupling. Since the system of simultaneous algebraic equations that results from this direct coupling method is unsymmetrical, the method is sometimes referred to elsewhere in the literature as unsymmetrical coupling.

Two small planar elastostatic problems were used in a limited numerical study of the coupled solution method. The first problem involved the stretching of a rectangular plate, and the second problem involved a pressurized circular cavity within the plane of an infinite elastic domain.

CONCLUSIONS

1. There are two approaches to the coupling of finite element and boundary element methods. One approach is to treat the finite element domain to appear as if it is a boundary element domain to the adjacent boundary element domain. The second approach is to treat the boundary element domain to appear as if it is a finite element (super element) domain to the adjacent finite element domain. We choose the former approach. We believe that this is the more effective approach when the combined system is computationally dominated by a boundary element domain.
2. Computed stress distributions across the interface between the two subdomains, one of finite extent and the other of infinite extent, were relatively smooth considering that both element formulations were of the lowest order. The constant boundary element would be adequate for semi-infinite and infinite domain problems in which the BEM subdomain is used to model the infinite domain but not expected to provide exceptionally

accurate results near the interface. We believe that higher order boundary elements would provide better local results near the interface of the two subdomains.

3. The computer code implementation of the direct coupling method is straightforward and, for the small problems investigated, the solution of an unsymmetrical system of equations posed no problem.

4. Some execution time comparisons were recorded that show the indirect boundary element method to be a considerably slower stress analyzer than the finite element method. For equal (but finite) subdomains, the boundary element method will account for the majority of the execution time in a coupled solution approach.

RECOMMENDATIONS

From the results of this study, the authors believe that a combined finite element and boundary element computer program could reduce the high cost now associated with nonlinear finite element programs. Further work is needed to make the BEM more effective. The areas requiring further investigation are:

- (1) Higher order (isoparametric) boundary elements.
- (2) Symmetric modeling capability. This requires elements that allow for either displacement or traction boundary conditions in either direction or an algorithm that incorporates lines of symmetry.
- (3) Body forces within the BEM region.
- (4) Effective equation solvers for block-banded nonsymmetric systems.
- (5) Development of symmetric BEM equations.

To better determine the potential of the BEM in reducing nonlinear FEM cost, a more accurate boundary element must be developed. A quadratic, isoparametric boundary element would allow a better evaluation of accuracy capability and the associated cost of problems involving a BEM region. The authors recommend that the theoretical and numerical treatment of isoparametric boundary elements be investigated.

REFERENCES

Atluri, S.N., and Grannell, J.J. (1978). Boundary element methods (BEM) and combination of BEM-FEM, Center for the Advancement of Computational Mechanics, School of Civil Engineering, Georgia Institute of Technology. Atlanta, Ga., Nov 1978.

Banerjee, P.K., and Butterfield, R. (1981). Boundary element methods in engineering science, Chapter 14. London, England, McGraw-Hill Book Co., Ltd., 1981.

Bathe, K.J., and Wilson, E.L. (1976). Numerical methods in finite element analysis, Chapter 6. Englewood Cliffs, N.J.; Prentice-Hall, Inc., 1976.

Beer, G. (1983a). "Infinite domain elements in finite element analysis of underground excavations," International Journal for Numerical and Analytical Methods in Geomechanics, vol 7, 1983, pp 1-7.

Beer, G. (1983b). "Finite element, boundary element and coupled analysis of unbounded problems in elastostatics," International Journal for Numerical Methods in Engineering, vol 19, no. 4, Apr 1983.

Beer, G., and Meek, J.L. (1981). "The coupling of boundary and finite element methods for infinite domain problems in elasto-plasticity," in Boundary Element Methods, in Proceedings of the Third International Seminar, C.A. Brebbia, Editor, Irvine, Calif., Jul 1981.

Bettess, P. (1977). "Infinite elements," *International Journal for Numerical Methods in Engineering*, vol 11, 1977, pp 53-64.

Brebbia, C.A. (1978). *The boundary element method for engineers*. London, England, Pentech Press Limited, 1978.

Brebbia, C.A., and Georgiou, P. (1979). "Combination of boundary and finite elements in elastostatics," *Applied Mathematical Modeling*, vol 3, 1979.

Bruch, J.C., Jr., and Zyvoloski, G. (1973). "Finite element solution of unsteady and unsaturated flow in porous media," in *The Mathematics of Finite Elements and Applications*, J.R. Whitman, Editor. New York, N.Y., Academic Press, 1973, pp 201-211.

Chen, H.S., and Mei, C.C. (1974). "Oscillations and wave forces in a man-made harbor in open sea," 10th Naval Hydro, Symposium, Department of Civil Engineering, Massachusetts Institute of Technology, Cambridge, Mass., 1974.

Fellipa, C.A. (1981). "Interfacing finite element and boundary element discretizations," in *Boundary Element Methods*, in *Proceedings of the Third International Seminar*, C.A. Brebbia, Editor, Irvine, Calif., Jul 1981.

Fellipa, C.A., Geers, T.L., and DeRuntz, J.A. (1974). Response of a ring-stiffened cylindrical shell to a transient acoustic wave, Office of Naval Research, Structural Mechanics Laboratory, Contract Report LMSC-D403671. Palo Alto, Calif., Lockheed Palo Alto Research Laboratory, 1974.

Gallagher, R.H. (1975). *Finite element analysis -- Fundamentals*. Englewood Cliffs, N.J., Prentice-Hall, Inc., 1975.

Kelly, D.W., Mustoe, G.G.W., and Zienkiewicz, O.C. (1979). "Coupling of boundary element methods with other numerical methods," Chapter 10 in *Developments in Boundary Element Methods*, P.K. Banerjee and R. Butterfield, Editors. London, England, Applied Science Publishers, 1979.

Lean, M.H., Friedman, M., and Wexler, A. (1979). "Application of the boundary element method in electrical engineering problems," Chapter 9 in *Developments in Boundary Element Methods*, P.K. Banerjee and R. Butterfield, Editors. London, England, Applied Science Publishers, 1979.

Mote, C.D. (1971). "Global-local finite element," *International Journal for Numerical Methods in Engineering*, vol 3, 1971, pp 565-74.

Mustoe, G.G.W. (1979). *Coupling of boundary solution procedures and finite elements for continuum problems*, Ph D thesis, University of Wales, University College. Swansea, Wales, 1979.

Shaw, R.P. (1974). "Time harmonic scattering by obstacles surrounded by an inhomogeneous medium," *Journal of the Acoustics Society of America*, vol 56, no. 5, 1974, pp 1437-1443.

Shaw, R.P. (1978). "Coupling boundary integral equation method to other numerical techniques," paper presented at *International Symposium on Recent Advances in Boundary Element Methods*, Southampton, Jul 1978.

Shaw, R.P. (1979). "Boundary integral equation method applied to wave problems," Chapter 6 in *Developments in Boundary Element Methods*, P.K. Banerjee and R. Butterfield, Editors. London, England, Applied Science Publishers, 1979.

Shaw, R.P., and Falby, W. (1978). "FE-BIE combination of the finite element and boundary integral method," *Journal of Computers and Fluids*, vol 6, 1978, pp 153-160.

Shugar, T.A., and Cox, J.V. (1983). Investigation of the indirect boundary element method in one- and two-dimensional elastostatics, Naval Civil Engineering Laboratory, Technical Note N-1664. Port Hueneme, Calif., May 1983.

Zienkiewicz, O.C., Bettess, P., and Kelly, D.W. (1978). "The finite element method for determining fluid loadings on rigid structures, two- and three-dimensional formulations," Chapter 4 in Numerical Methods in Offshore Engineering, O.C. Zienkiewicz, R.W. Lewis, and K.G. Stagg Editors. New York, N.Y., John Wiley and Sons, 1978.

Zienkiewicz, O.C., Kelly, D.W., and Bettess, P. (1977). "The coupling of the finite element method and boundary solution procedures," International Journal for Numerical Methods in Engineering, vol 11, 1977, pp 355-375.

Table 1. A Comparison of Boundary Element Method (BEM) and Finite Element Method (FEM) Solution Times for Coupled Analysis

Operation Step	BEM Subdomain	FEM Subdomain
1. Develop the system of equations	11.25 min	6.5 min
2. a. Insert the system in the coupled system	6.25 min	2.25 min
b. Solve coupled system (order 82)	30.5 min	
3. Calculate responses: For a single point/element		
Displacement	16 sec	N/A
Stress	16 sec	3.5 sec
Combined	25 sec	
For the field	16.2 min	3.2 min

Table 2. Stress Comparison for Axially Loaded Plate

Finite Element Number	Finite Element Stress - Loaded End to Interface (psi)	Boundary Element Stress - Restrained End to Interface (psi)	Percent Difference
1	1.000	1.110	--
2	1.001	1.018	--
3	1.000	0.972	--
4	1.000	0.983	--
9	0.999	0.937	6.4
10	1.001	0.970	3.1
11	1.001	1.006	0.5
12	1.000	1.010	1.0
17	1.001	0.946	6.4
18	1.002	0.969	3.3
19	1.002	0.999	0.3
20	0.995	1.005	1.0
25	1.026	0.952	7.5
26	1.001	0.984	1.7
27	0.984	0.997	1.3
28	0.989	0.995	0.6

Table 3. Radial Stress Results in the Cavity Problem

Distance from Cavity Center (ft)	Elasticity Theory (psi)	Coupled BEM-FEM 12-BE, 24-FE (psi)		Direct BEM, 24-Element (psi)	Indirect BEM (psi)	
		Model 1	Model 2		24-Element	12-Element
4	-56.25	-60.49	-62.59	-57.24	-58.86	-60.52
6	-25.00	-26.05	-29.94	-25.29	-26.18	-27.03
10	-9.00	-9.38	-9.70	-9.11	-9.42	-9.73
20	-2.25	-2.34	-2.42	-2.28	-2.35	-2.43
50	-0.36	-0.375	-0.388	-0.364	-0.377	-0.389
200	-0.0225	-0.0234	-0.0242	-0.0228	-0.0237	-0.0246
1,000	-0.0009	-0.00094	-0.00097	-0.00091	-0.0027	-0.00126

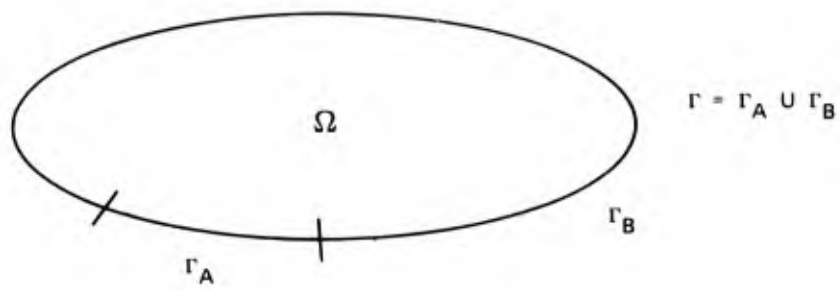


Figure 1. Domain of the differential equation.

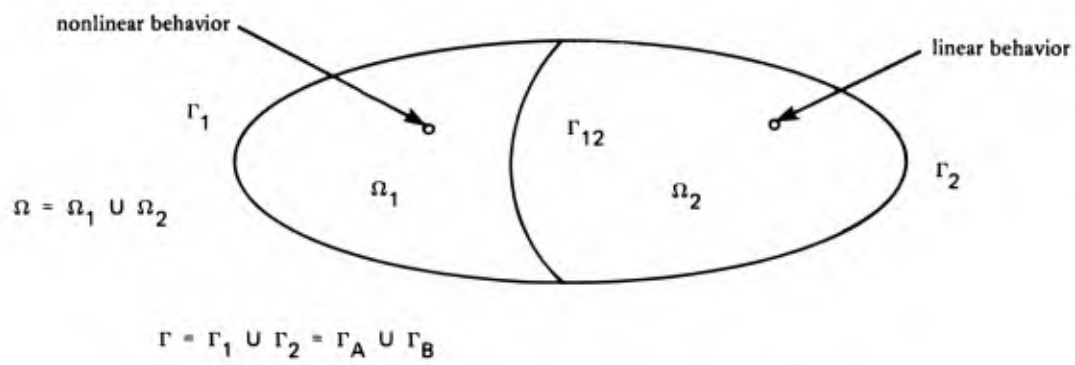


Figure 2. The subdivided domain.

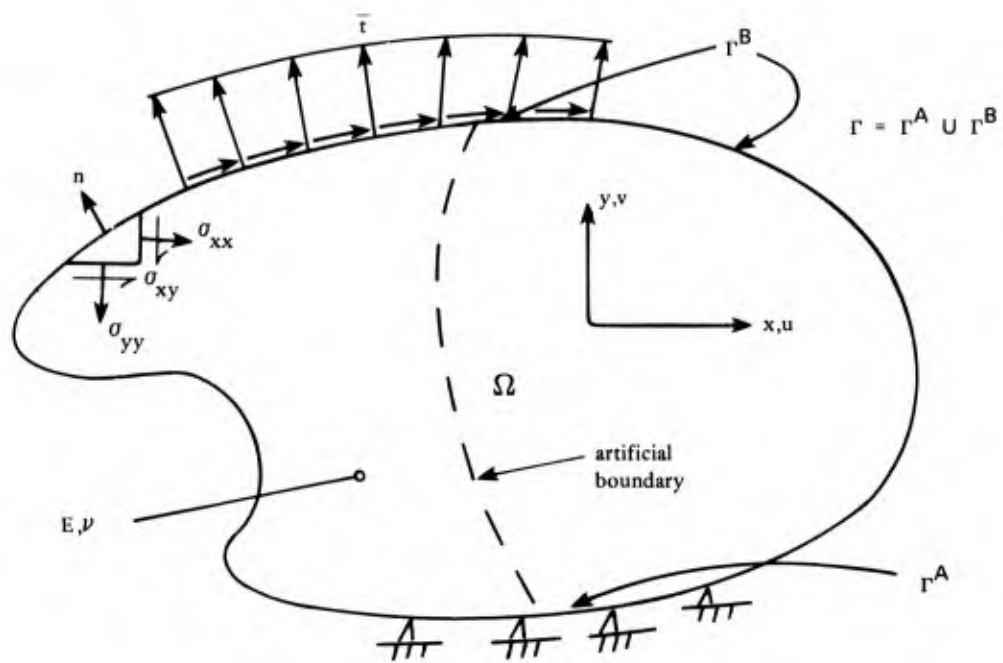


Figure 3. Two-dimensional elastostatics problem.

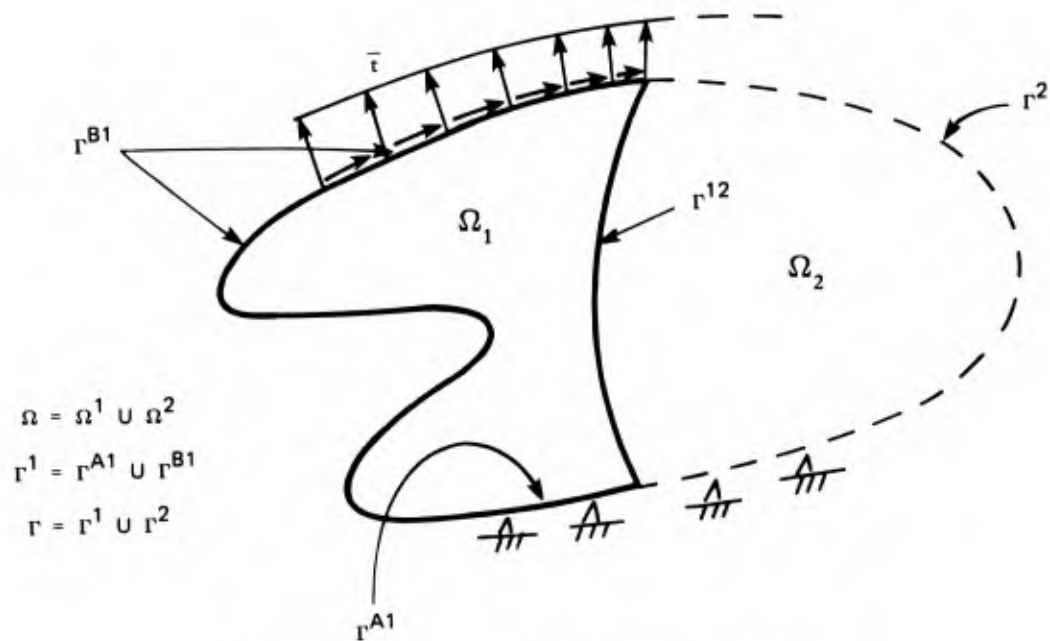


Figure 4. The finite element subdomain.

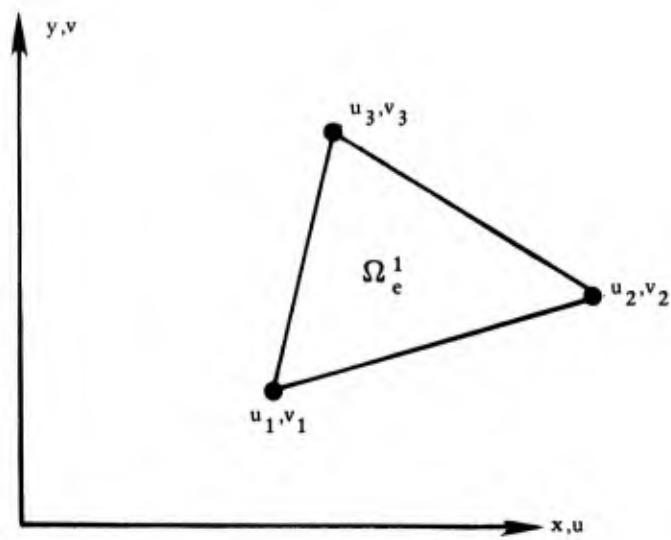


Figure 5. Triangular subdivision of Ω^1 .

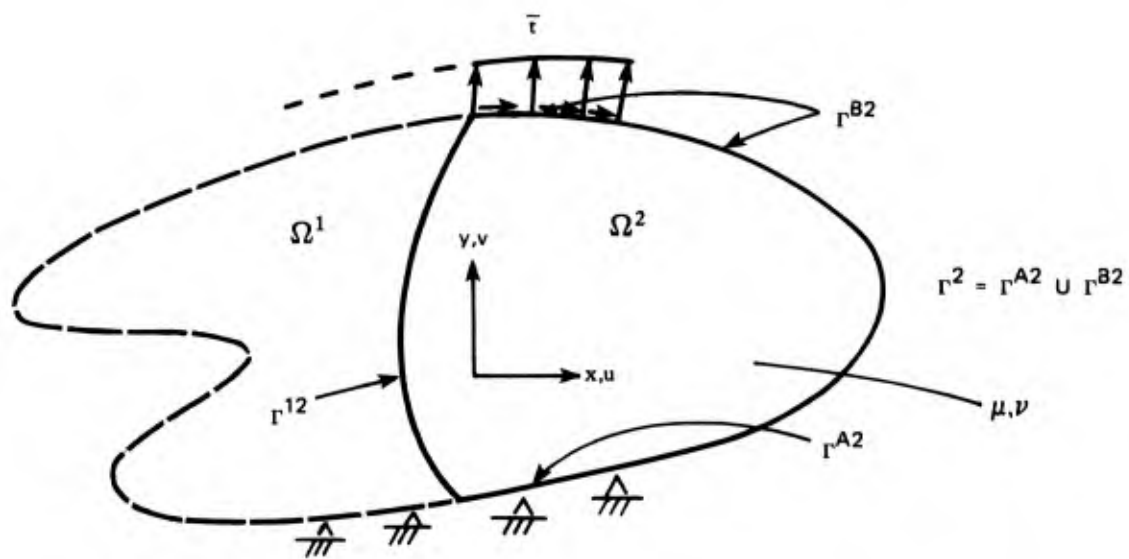


Figure 6. The indirect boundary element subdomain.

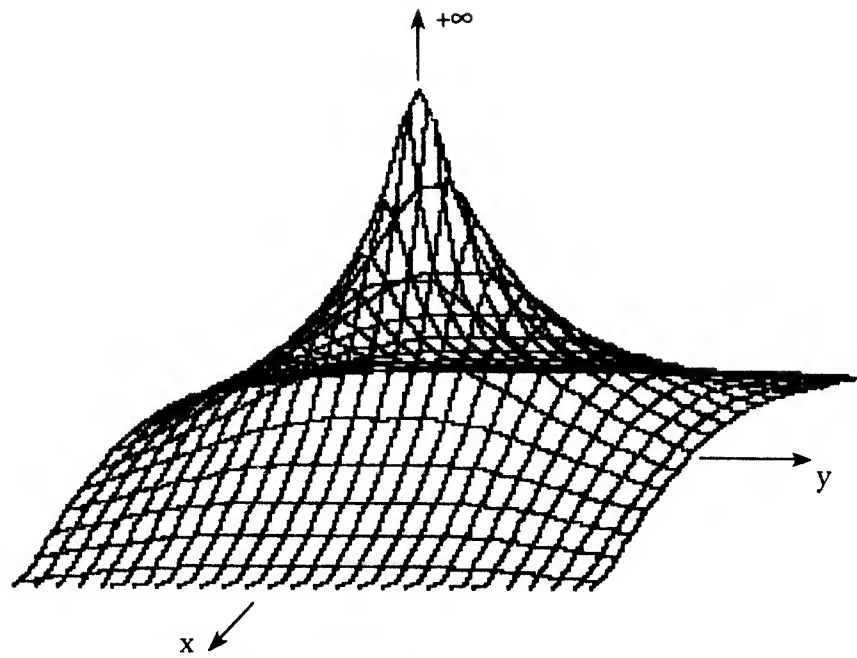


Figure 7a. Weakly singular function.

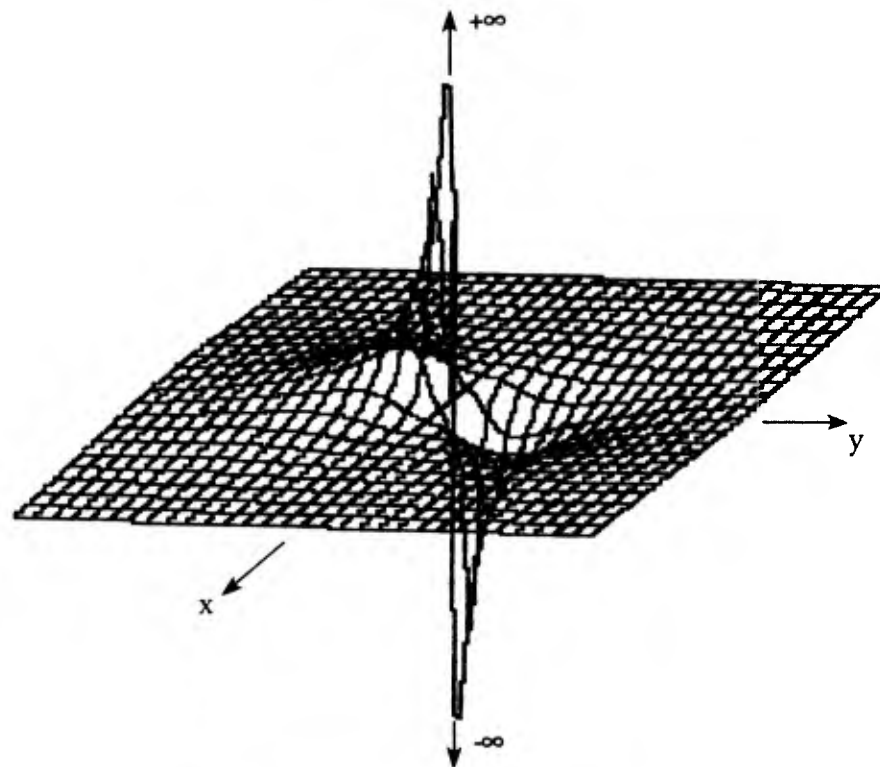


Figure 7b. Strongly singular function.

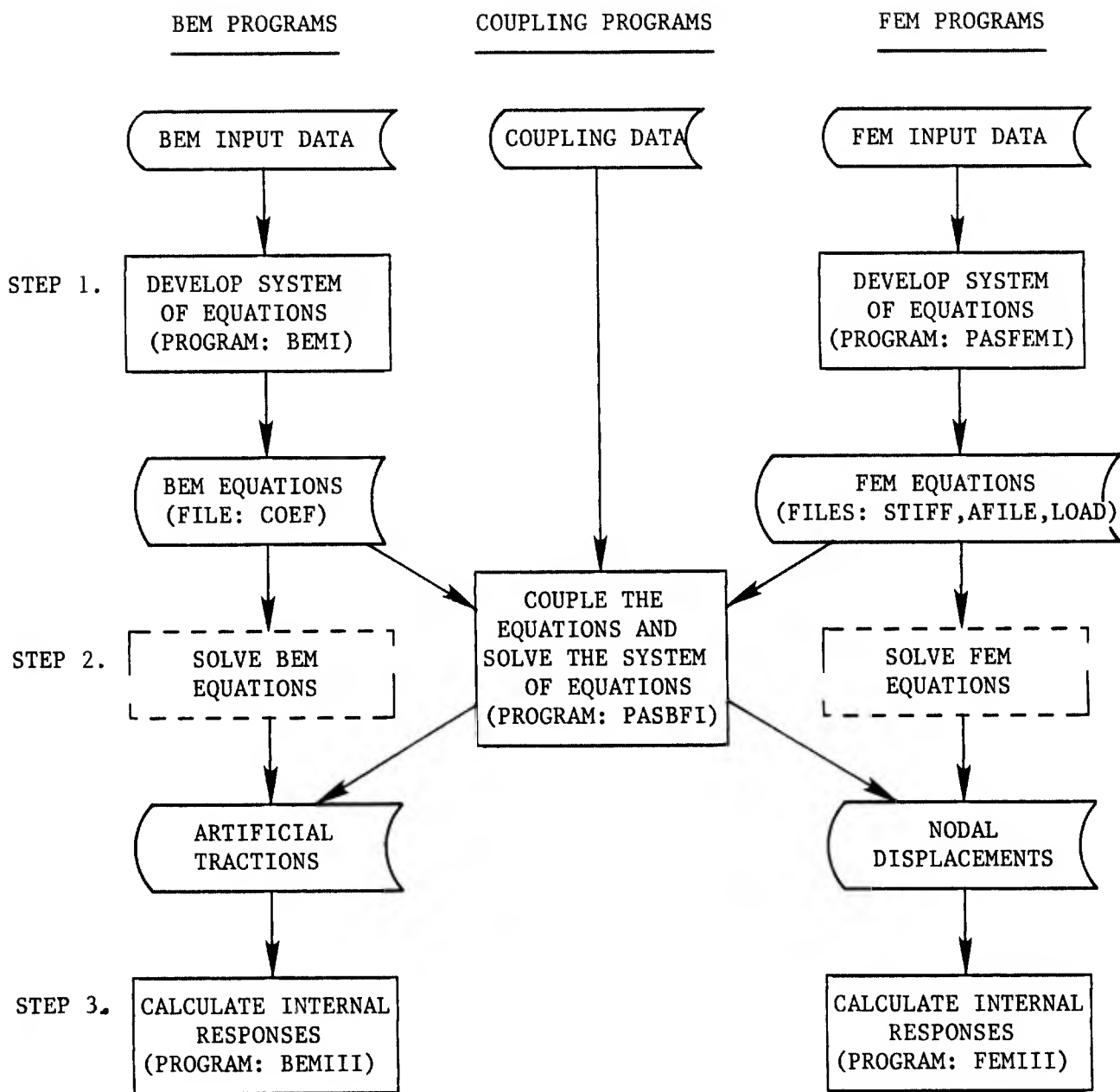


FIGURE 8. MODULAR COUPLING OF FEM AND BEM PROGRAMS.

POPULATION OF SYSTEM zero tolerance of 1.00000E-30

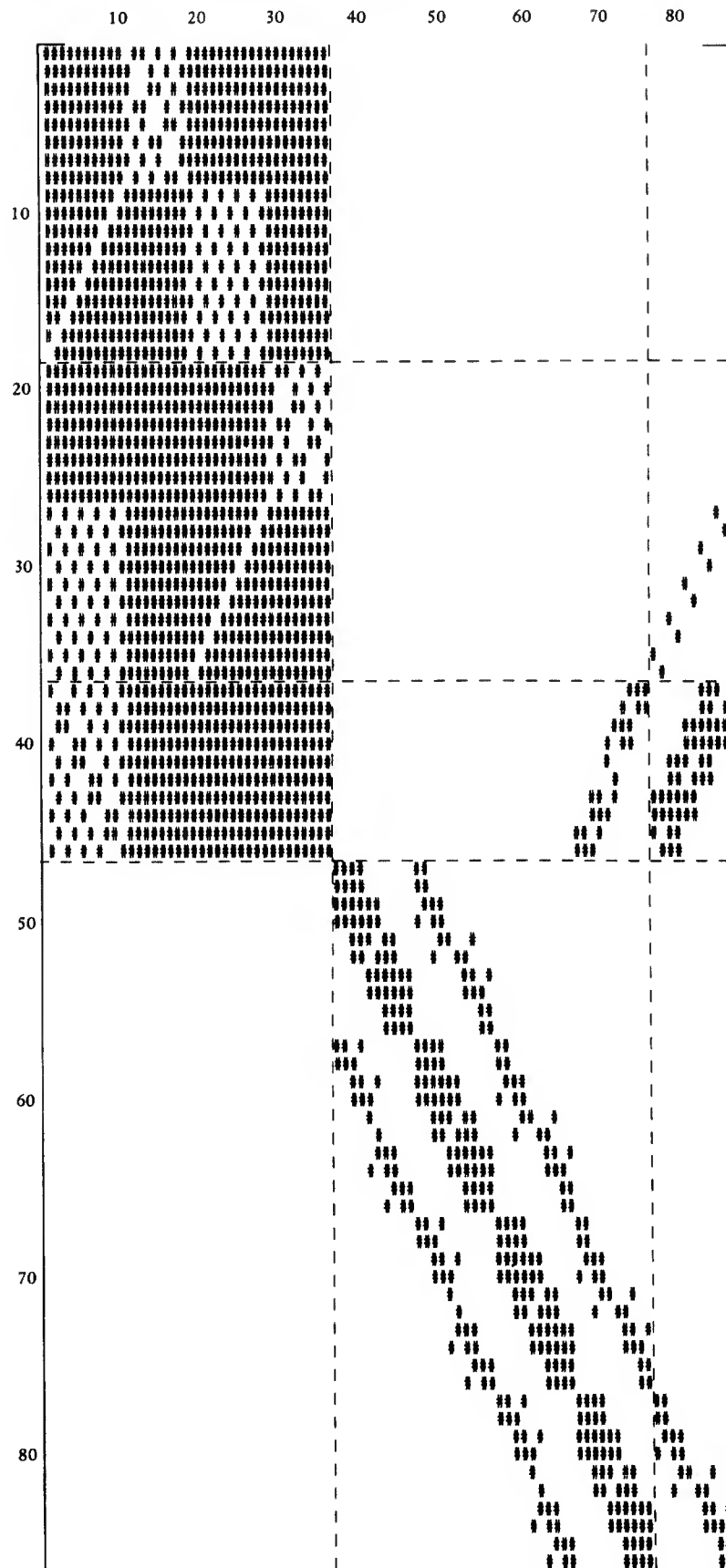


Figure 9. Population of coupled system matrix in Equation 19.

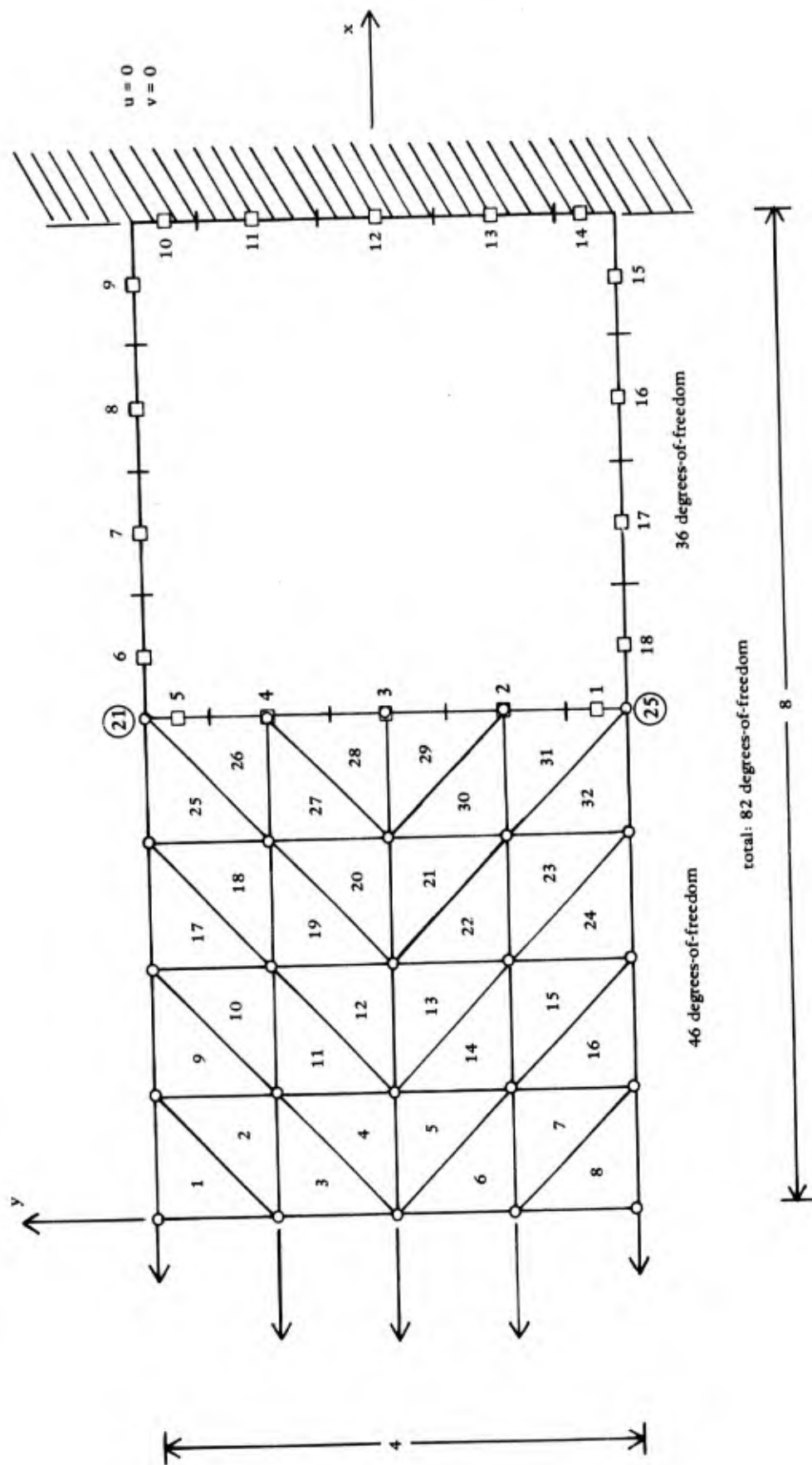
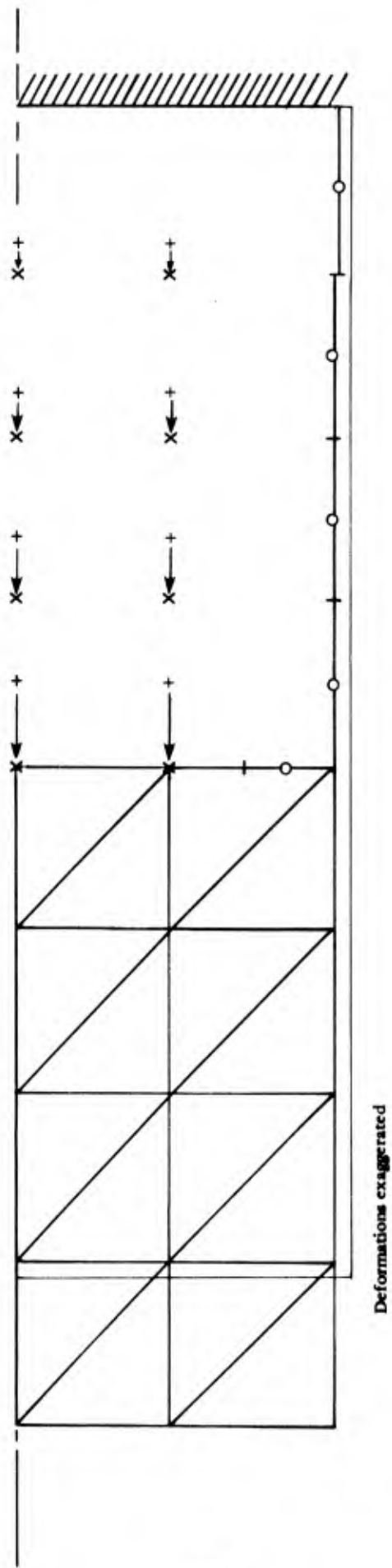


Figure 10. Axially loaded plane stress model.



Deformations exaggerated

Figure 11. Displacements in the axially loaded membrane.

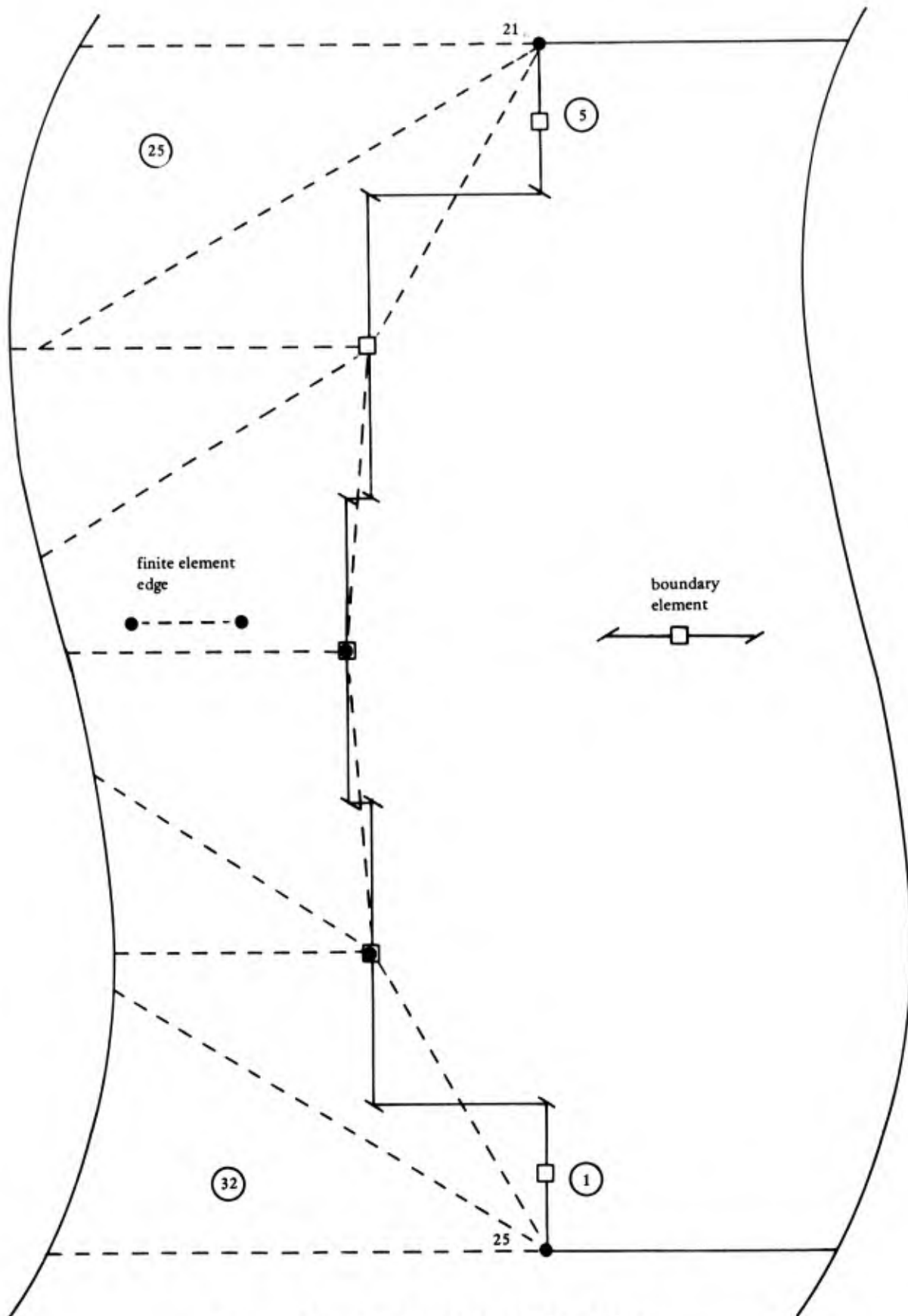


Figure 12. Deformation at interface.

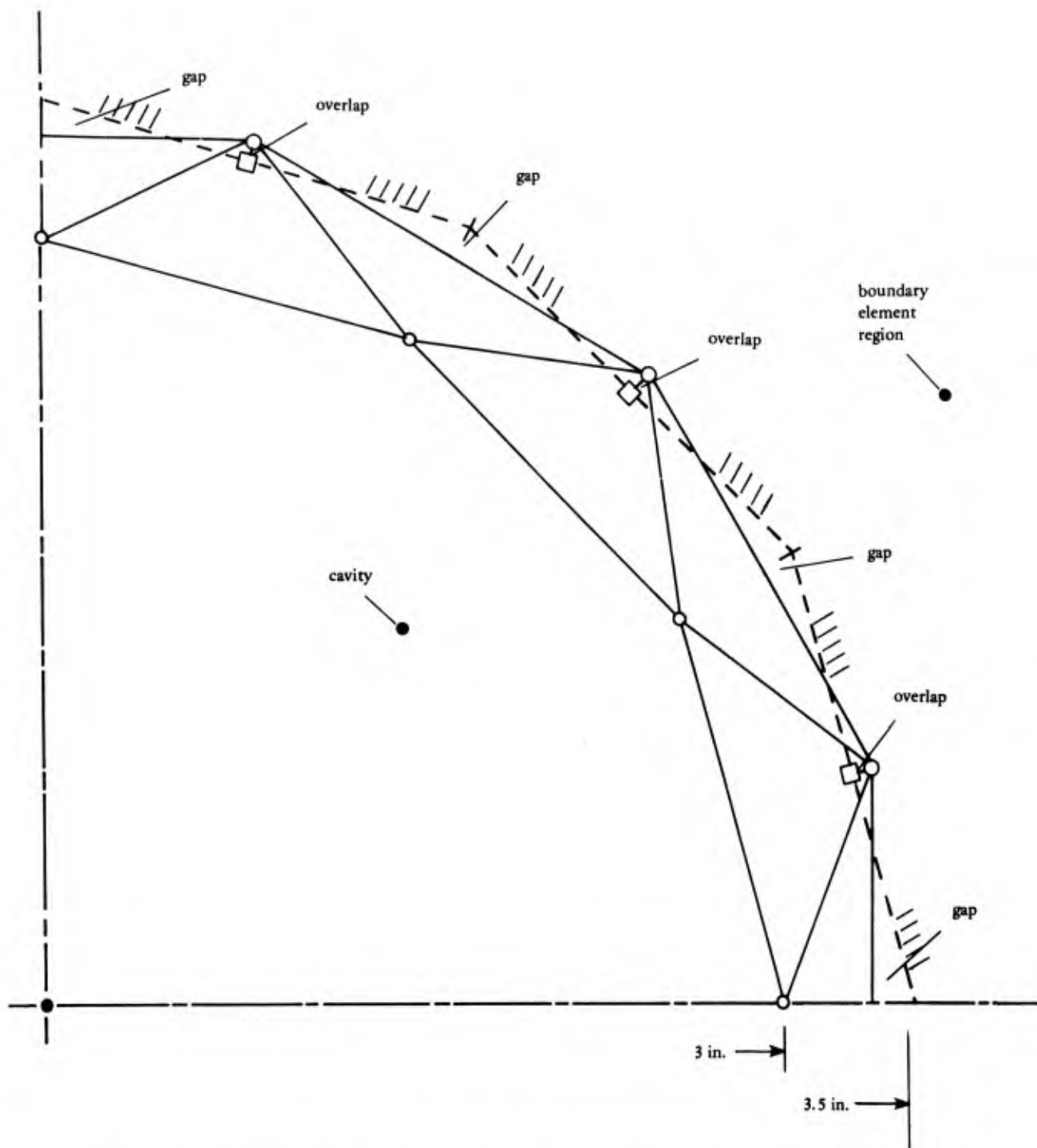


Figure 13. Cavity in an infinite medium, one-quarter of model 1.

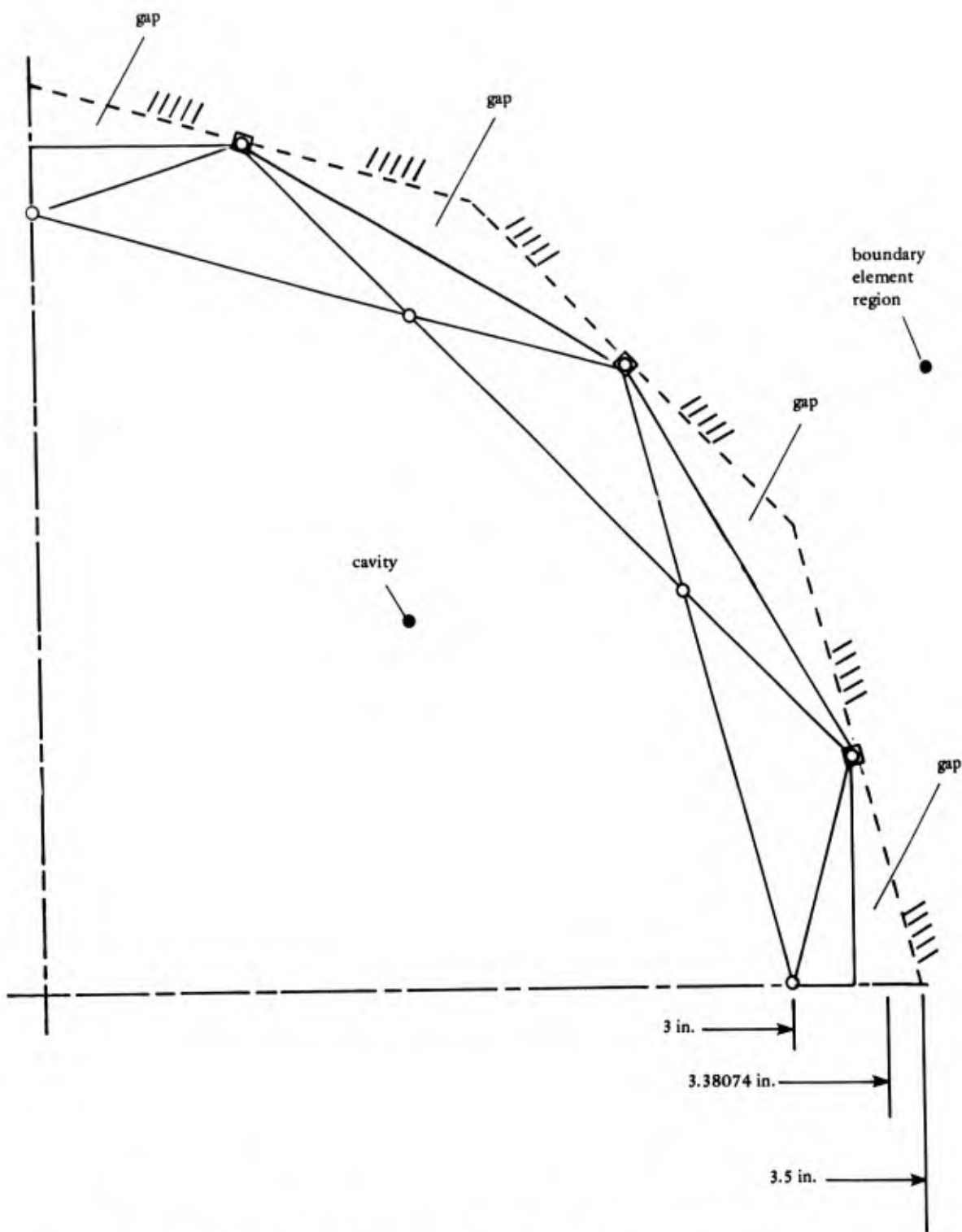


Figure 14. Cavity in an infinite medium, one-quarter of model 2.

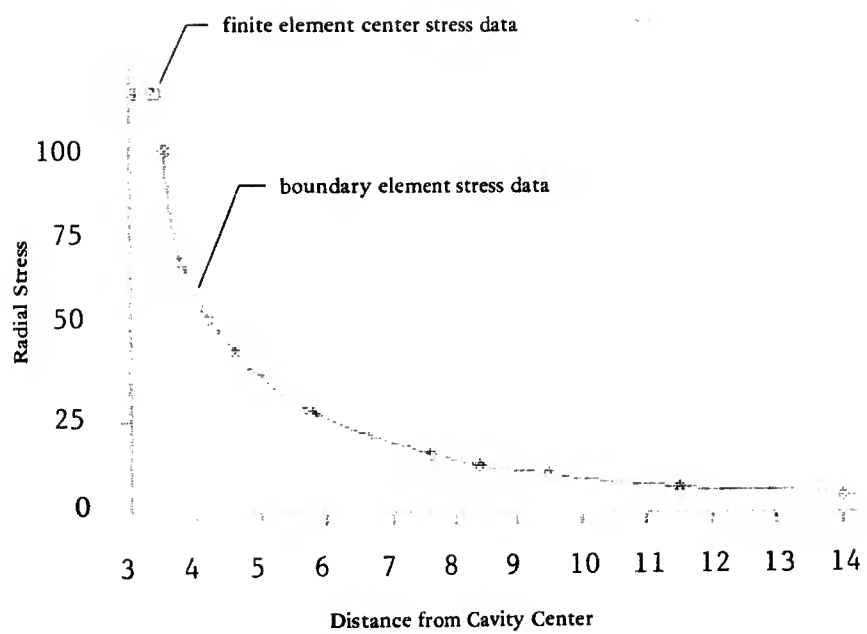


Figure 15. Radial stress versus distance for "cavity problem."

Appendix A

BOUNDARIES AND BOUNDARY CONDITIONS IN THE FINITE ELEMENT MODELING OF SOILS

The problem being addressed is of a very practical nature in solving semi-infinite media problems (soil, rock) by the finite element method. Its solution may be somewhat case-dependent, but in all cases it must be reckoned with to at least some degree.

Difficulty always exists in determining the extent of surrounding media to be included in a finite element model whose dimensions are necessarily finite, at least that is the case at present.* In addition, what selection of boundary conditions should be made; should they be completely fixed, completely free, or partially constrained?

The solution is to run a number of analyses with differing finite element model size until further increases in extent make little difference in the information considered most important: displacements, stress, etc. This is a costly operation, but unless accomplished, the analysis is open to criticism. Further, if it is not a one-shot analysis, the smallest domain consistent with the desired accuracy may be desirable from an economic standpoint.

An analysis of the vertical deflection of a simple elastic soil mass will help illustrate the solution dependence on geometrical extent. The problem and its solutions are shown in Figure A-1.

*Semi-analytic finite element methods, such as the global-local concept, may, with further development, provide workable codes where only a portion of the semi-infinite media need be discretized while the remainder is characterized by appropriate orthogonal functions in the classical Ritz sense.

For any given depth ℓ of geometrical extent, an assumed uniform strain distribution (along any horizontal section) can be integrated to find the deflection u . Obviously, the solution u is dependent on ℓ , the geometrical extent factor in the problem.

Imagine, for a moment, that $\lim u$ was not known. Now the equation must be solved for several trial values of ℓ and the results must be plotted until further solutions provide little change in the displacement to be sure that the geometrical extent ℓ is sufficiently great that convergence has been achieved.

While this problem is almost trivial, it nevertheless illustrates exactly what happens when applying the finite element method to semi-infinite soil problems. A single finite element model of the media is no more sufficient than is one value of ℓ to establish reliable results. A convergence study must be accomplished by several trial finite element model solutions, each with a different geometrical extent in the semi-infinite media.

The elastic model illustrates one other point that is also applicable to finite element models. Since $\lim u$ is a function of $\cot \alpha$, the limit does not exist for $\alpha = \pi/2$. This means that the convergence study must be posed properly by allowing expansion of geometrical extent in both the horizontal and vertical directions simultaneously. Otherwise the convergence study is ill-posed; in most cases convergence to erroneous values will occur, and in others the solution may be unbounded.

Convergence studies of this nature were necessary for a nonlinear, axisymmetric analysis of repaired bomb craters in runways. The particulars are not important, but the finite element model was to simulate small-scale field tests of repaired craters. Surface deflections were the criterion on which the convergence study was based.

Three geometrical techniques for achieving convergence were studied:

- (1) Dual expansion--both width and depth expanded.
- (2) Single expansion on width--depth constant.
- (3) Single expansion on depth--width constant.

In Figure A-2, maximum vertical centerline displacement is plotted against a geometry parameter C , which may represent either the width or the depth or both depending on the technique being studied. Each point represents a complete computer run.

Though the boundary condition along the outer edge was also studied, concentrate for now on the three solid curves (a fixed edge condition). The two single expansion concepts, the lower two curves, tend to converge prematurely. But the dual expansion technique indicates the true deflection to be much higher and, while convergence has not as yet been achieved, it is imminent.

Looking at the three dashed curves (a roller edge condition), it can be seen that one of the two single expansion techniques refuses to converge and the other tends to converge prematurely. The dual expansion technique again indicates imminent convergence.

Before carrying the convergence study further, the influence of the vertical edge condition can be seen by comparing the dashed and solid curves for the dual expansion technique. In theory both curves should converge monotonically to the same value because when C is infinite the edge condition should not matter. Based on that, the roller edge condition converges faster and therefore is the choice over the fixed edge.

The study was continued using only the dual expansion technique. The same kind of data is shown in Figure A-3, except the geometry parameter is extended farther. Little is to be gained by extending beyond 500 inches, so that at this point the study was terminated (about a 12% difference in the highest and lowest curves exists). An argument can probably be made for adopting any of the curves. Nevertheless, the inclination is to choose the middle two curves as they are flatter over a longer distance.

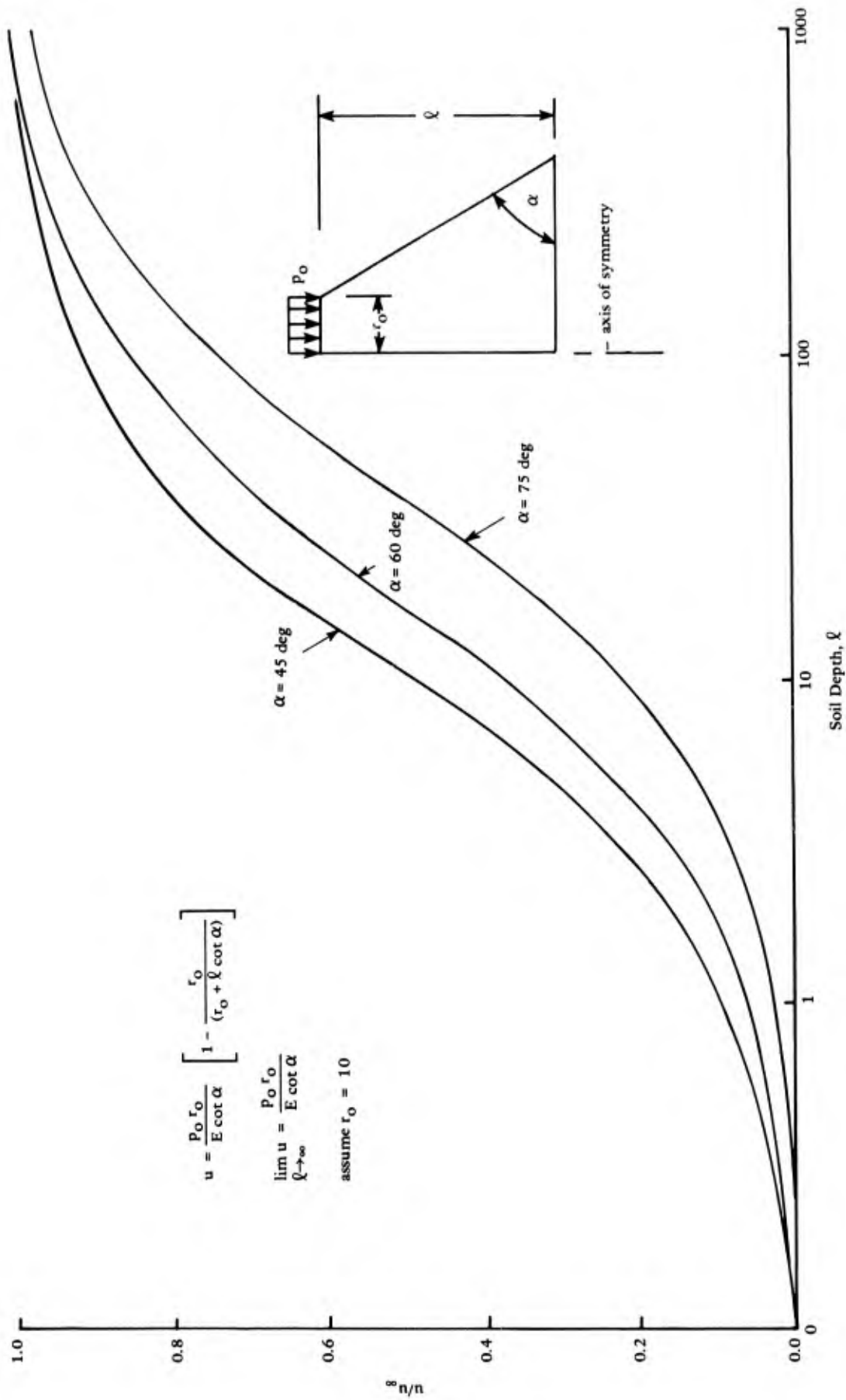


Figure A-1. Convergence of centerline vertical deflection.

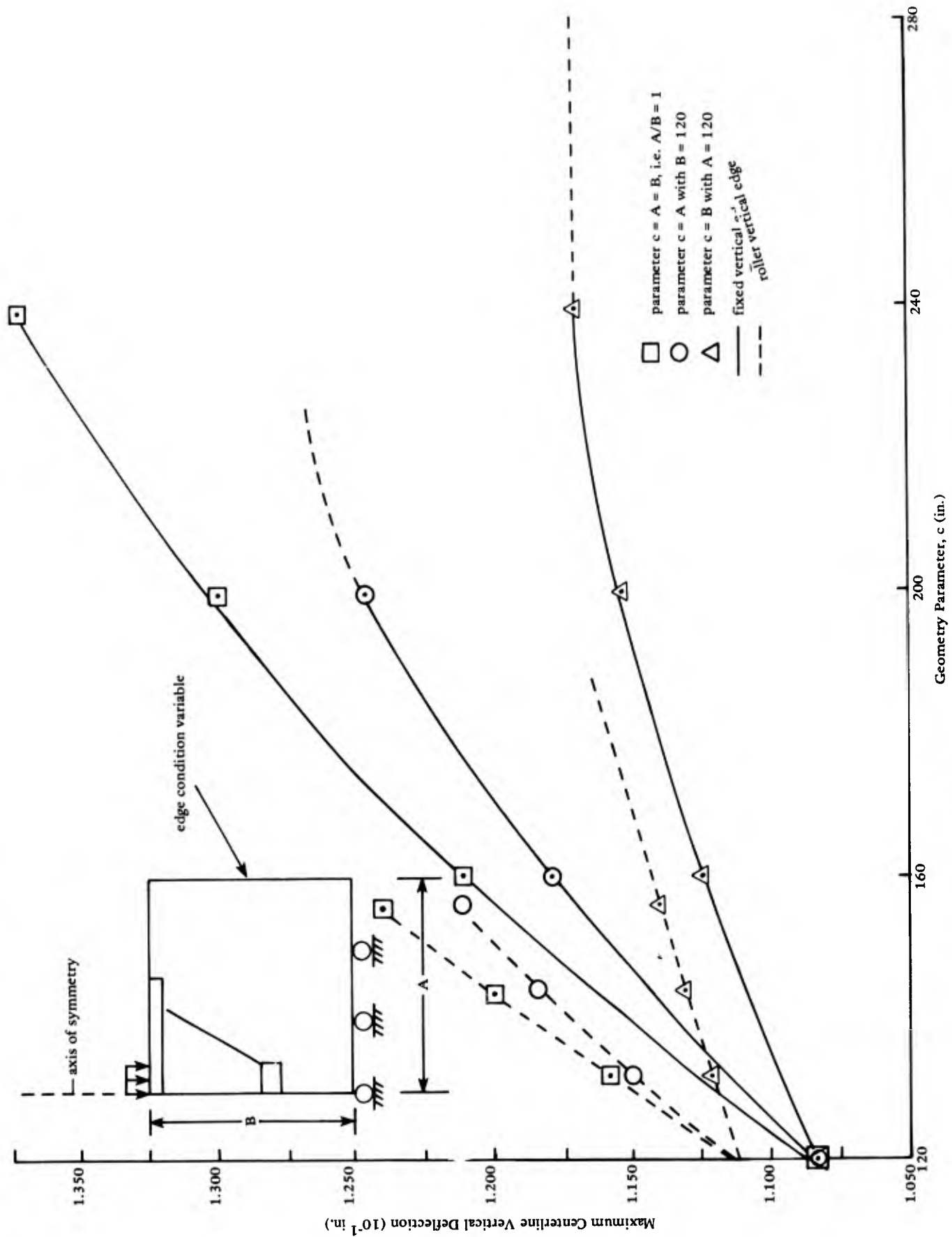


Figure A-2. Convergence study of semi-infinite media idealization models.

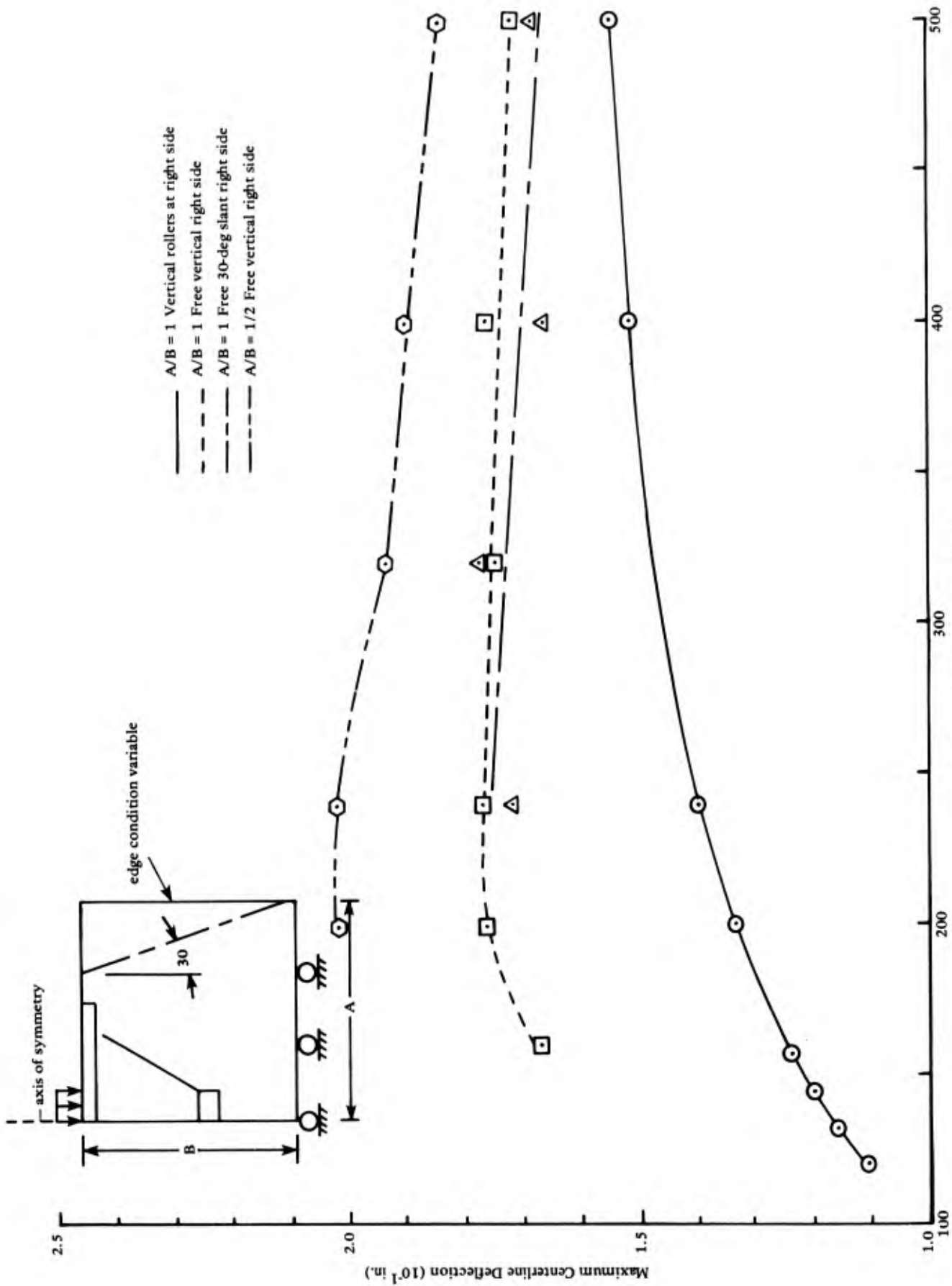


Figure A-3. Convergence study using dual expansion concept.

Appendix B

ASPECTS OF THE FINITE ELEMENT IMPLEMENTATION

The finite element program (PASFEM) used in this study is a static, two-dimensional, linear, finite element code. The initial version only contains a constant strain triangular element. Part of the program design parallels the methodology presented by Bathe and Wilson (1976). The emphasis in this appendix is on the design decisions related to assembly of the finite element method (FEM) system of equations.

Part of the "bookkeeping" involved in assembling the FEM system of equations consists of relating element degrees-of-freedom (DOF) to system DOF. There are three important arrays involved in this process. An identification array (ID) of dimension "number DOF per node" by "number of nodes" relates nodal DOF to system DOF. For the two-dimensional problems being considered, the "number DOF per node" equals three: two translations and one rotation.

There are two steps in defining the ID array. The first step is to flag the restrained degrees of freedom. Most FORTRAN finite element codes flag the restrained degrees-of-freedom with a "1" in the array. This convention is based on the form of the formatted input data, where a "1" is placed in a field if the corresponding degree-of-freedom is to be restrained. The Pascal language does not include formatted input, and a more self-documented data file is preferred. Flagging the free degrees-of-freedom with a "1" results in less effort since a replacement, in the second step, is only performed at the free DOF. The second step in the definition of the array then involves scanning the columns and replacing "1"s with successively larger integers.

Another important array in the assembly of the FEM system of equations contains the connectivity of the elements (a list of nodes the elements are connected to) and the element material numbers. This information is easily read into the array ICONN from the data file. In PASFEM, ICONN is present in memory one row (element) at a time. The developed algorithm requires ICONN to be read once when establishing the skyline and once when calculating the element stiffness matrix and assembling it into the structure stiffness matrix.

With the ID and ICONN arrays, the element DOF can be related directly to the system DOF. This relationship is the basis of the ICODE array (Bathe and Wilson's LM array). Each column of ICODE corresponds to an element and each row corresponds to an element DOF. For example in the two-dimensional code, ICODE(2,15) would contain the system DOF number for the second element DOF (node-a's y-translation) of the 15th element. As with ICONN, in the PASFEM program, ICODE is present in memory one element at a time.

PASFEM uses the skyline storage scheme to store the structure stiffness matrix in a one-dimensional array, A. An essential part of this scheme is the pointer array MAXA. The *i*th term in MAXA points at the A array location of the *i*th diagonal term of the K matrix.

PASFEM is probably closer to ADINA than SAP in the structure stiffness matrix assembly. The first call to the element routine calculates ICODE and updates the skyline. With MAXA developed the second call to the element routine calculates the compact element stiffness matrix and immediately adds it to the structure stiffness matrix. The assembly process design is based solely on the consideration outlined in the following paragraphs.

In a "SAP-like design" the element stiffness matrix is kept on backup storage (disk in this case). The first call to the element routine calculates the element stiffness matrix and writes it to disk. The second call then reads the element stiffness matrix and sums it into the structure stiffness matrix. With the simple constant strain triangle (CST) element this results in 21 writes and 21 reads for the upper triangular stiffness matrix. In general, the number of input/output (I/O) operations is slightly larger than the square of the number of

element DOF. To increase the amount of high-speed memory available for the structure stiffness matrix, additional I/O operations are required to force ICONN and ICODE to reside in memory one element at a time. For a two-dimensional code, this results in approximately 2.5 times the number of element DOF, I/O operations.

The design used for the PASFEM program does not involve any I/O operations related to element stiffness matrix storage. The only I/O operations are involved with requiring ICONN and ICODE to be resident one element at a time. The disadvantage of this design is that the nodal coordinates, material properties, and section properties are resident in memory during the assembly of the stiffness matrix. Thus, the I/O operations related to ICONN and ICODE are more of a necessity.

Appendix C

COUPLING ALGORITHM

The equations are coupled exactly in the form shown in Equation 19. The following explains the algorithms used to couple the equations by presenting the algorithms in a structured pseudo-code or Pascal.

Before explaining the algorithm, the form of the boundary element method (BEM) and finite element method (FEM) equation and coupling data files must be understood. The first BEM program (BEMI) of Figure 8 creates a data file that consists of a full matrix of coefficients, while the first FEM program (FEMI) creates a data file that consists of the coefficient matrix stored in a "skyline" manner (Bathe and Wilson, 1976).

The BEM equations are developed two rows at a time, corresponding to the two known boundary values at each constant element. The BEM INPUT DATA file indicates whether each element has known boundary displacements, tractions, or if it is an interface element. Known boundary displacement elements result in BEMI generating two rows of \underline{G}^{A2} (Equation 8); known boundary tractions result in BEMI generating two rows of \underline{F}^{B2} (Equation 10). Hence, interface elements result in BEMI generating two rows of \underline{G}^{12} and \underline{F}^{12} (Equations 9 and 11, respectively). BEMI writes the equations to the disk file COEF as they are developed so that this first program is not "memory limited." Each set of linear equation coefficients is prefaced by a flag indicating which boundary values are known. The coefficients are written to the disk in blocks of four terms, corresponding to the relationship between the artificial boundary tractions at one element and the known boundary values at another element. The corresponding boundary values are written to the file for noninterface elements.

The development of the FEM equations is performed one element at a time. Some aspects of the implementation are explained in Appendix B. The stiffness matrix is written to the disk file STIFF as a one-dimensional array, stored in a skyline manner. Each column of terms is prefaced by the number of terms in the given column and the pointer array (MAXA) value. In addition to the STIFF file two other files associated with the FEM program are needed by the interface program. The AFILE file contains coordinate data, the ID array, and material properties. The LOAD file contains the nodal load vector.

The coupling data file simply provides for the connectivity between the BEM and FEM regions. This is the first file read by the coupling program. Each data item contains a boundary element (BE) number and a corresponding finite element (FE) node number (BE numbers must be listed in descending order in this implementation). Counting the data items gives the total number of interface nodes. The data are read into the two-dimensional array IFACE (see partial listing below).

```
BEGIN (the FACEIN procedure)
WRITELN('      Executing the FACEIN procedure');
RESET(INFACE, 'CEDATA:INTERFACE.TEXT');
N:=0;                {initialize the interface element number}
READLN(INFACE);      {skip the INFACE header}
READ(INFACE,LETTER); {read first letter of the next line}
REPEAT
  N:=N+1;            {increment the number of interface elements}
  WHILE LETTER='.' DO
    BEGIN
      READLN(INFACE);
      READ(INFACE,LETTER)
    END;
  READLN(INFACE, IFACE[N, BOUNDEL], IFACE[N, FEMNODE]);
  READ(INFACE, LETTER)
UNTIL EOF(INFACE)
END; (the FACEIN procedure)
```

Each row of IFACE represents an interface element: the first column contains the boundary element number and the second column represents the finite element node number. (Note that the second array indexes, BOUNDEL and FEMNODE, are not variables in this case. These are values of a user-defined data type, analogous to using 1 and 2 in the FORTRAN language. The advantage is that the Pascal code is closer to self-documented.)

With the coupling connectivity known, the boundary element equations are first placed in the coupled system. The submatrices associated with the boundary element system are relatively simple to insert in the coupled system as compared with inserting the finite element submatrices. The procedure INSERTBEM reads from the COEF file the number of boundary elements and the number of interface elements. These data do not provide enough information to determine the order of the coupled system; however, the position of the submatrices \underline{FG}^{AB} , \underline{G}^{12} , and $-\underline{EF}^{12}$ can be determined. The submatrix pointers are given by

```
POINTBOUND = 1
POINTCONT  = 2*(NUMBEL-NUMINTEL) + 1
POINTEQUAL = 2*(NUMBEL) + 1
```

where NUMBEL = the number of boundary element equations
 NUMINTEL = the number of interface boundary elements
 POINTBOUND = the pointer for the uncoupled BEM equations,
 \underline{FG}^{AB} and \underline{KBV} , set to 1 in this implementation
 POINTCONT = the pointer for the continuity equations, \underline{G}^{12}
 POINTEQUAL = the pointer for the equilibrium equations, $-\underline{E} \underline{F}^{12}$

With the above pointers determined, a set of rows can be read from the COEF file into the proper submatrix. The input loop for reading the boundary element equations is outlined as

```

FOR each element (1 to the number of elements)
  READ the known boundary condition
  IF the element is not an interface element
    THEN READ two equations of  $\underline{FG}^{AB}$ 
        increment POINTBOUND by 2
        READ two known boundary values of KBV

    ELSE READ two equations of  $-\underline{E} \underline{F}^{12}$ 
        increment POINTEQUAL by 2
        set the corresponding equilibrium  $\underline{Q}$  values to zero
        READ two equations of  $\underline{G}^{12}$ 
        increment POINTCONT by 2
        set the corresponding continuity  $\underline{Q}$  values to zero

next element

```

The above loop results in the completion of submatrices \underline{FG}^{AB} , \underline{G}^{12} , and $-\underline{E} \underline{F}^{12}$ in the coefficient matrix and the \underline{KBV} and \underline{Q} submatrices in the known vector of the system.

With the BEM system of equations placed in the combined systems, the FEM system is now coupled to it. Prior to this coupling some preliminary steps are required. The first step is to set pointers to the FEM submatrices. This is similar to the process performed for the BEM submatrices. The number of nodes (NUMNODE) and the number of equations (NUMEQ) are read from AFILE. Then submatrix pointers and the order of the final system of equations are given by

```

PFEMCOL = 2*NUMBEL + 1
PEQUAL = PFEMCOL
PFEM = PEQUAL + 2*NUMINTEL
ORDER = NUMBEL*2 + NUMEQ

```

where PFEMCOL = the column pointer for the FEM equations

PEQUAL = the row pointer for the equilibrium equations,

$\tilde{K}_{21} : \tilde{K}_{22}$

PFEM = the row pointer for the uncoupled FEM equations,

$\tilde{K}_{11} : \tilde{K}_{12}$

The second preparation step is to zero sections of the coefficient matrix. The remainder of the matrix consists of Q matrices and the sparse matrices \tilde{K} and \tilde{A} . The stiffness matrix is stored in a skyline manner on the disk and \tilde{A} is composed of negative identity vectors that are generated while reading \tilde{K} .

The last step required prior to inserting the FEM system is to relate the FEM equation numbers to the coupled system equation numbers. A pointer array, similar to the one used in relating element DOF to structure DOF in finite element implementations, handles the "book-keeping." This pointer array, NEWROW, gives the new row numbers of finite element stiffness terms. The column order of the system of equations does not change. The use of NEWROW allows the finite element equations to be read from the file and to immediately be placed in the system of equations. Since the coupling is nonsymmetric, each FEM stiffness term must be inserted into two locations of the coupled system.

NEWROW is developed in a three-phase process in the MAKENEWROW procedure. The final contents of the i th term in NEWROW give the row number of the coupled system into which the i th row of the finite element system are to be read.

The first phase of the development involves the finite element ID array (see Appendix B), which relates nodal DOFs to the system equation numbers. The first phase is outlined as

```

initialize the NEWROW index, ROW, to 1
FOR each finite element node (I)
  FOR each nodal degree-of-freedom (J)
    READ the J,I value of ID from AFILE
    IF the ID value is not zero
      THEN NEWROW[ROW] = I
        increment ROW by 1
  next nodal degree-of-freedom
next finite element

```

Following this phase, the NEWROW array contains the node number that corresponds to each structure DOF in the FEM system.

The second phase of the development replaces the node numbers in NEWROW of the interface elements with the negative of their equation numbers in the coupled system. The second phase is outlined as

```

FOR each interface element (I)
  initialize the NEWROW index, ROW, to 1
  set the NODEISFOUND flag to false
  REPEAT for each NEWROW value
    IF NEWROW[ROW] is the Ith interface node
      THEN set NODEISFOUND to true
        IF the next NEWROW value, ROW+1,
          corresponds to the same interface node
            THEN NEWROW[ROW+1]= -I*2 + 1 - PEQUAL
              NEWROW[ROW] = -I*2 + 2 - PEQUAL
        increment ROW by 1
  UNTIL NODEISFOUND
next interface element

```

where PEQUAL is equivalent to POINTEQUAL given earlier; however, in this loop the equilibrium equation point continues to point at the first equation of the equilibrium submatrices. Following this phase the NEWROW array contains the node numbers at noninterface nodes and the

negative equation numbers at the interface nodes. The final values for the interface nodes are now in the NEWROW array. The negative is used as a flag in the third phase of development to indicate the number is an equation number and not a FEM node number.

The final phase of the NEWROW development, which loops over all the NEWROW values replacing positive node numbers (noninterface elements) with equation numbers and switching negative equation numbers (interface elements), is outlined as

```
set I to PFEM, the pointer for the uncoupled FEM equations
```

```
FOR each FE equation (ROW)
```

```
  IF the NEWROW[ROW] value is positive
```

```
    THEN NEWROW[ROW] = I
```

```
      I = I + 1
```

```
  ELSE NEWROW[ROW] = -NEWROW[ROW]
```

```
next FE equation
```

The equation counter for noninterface nodes starts at PFEM and increments by one; thus, the \tilde{K}_{11} and \tilde{K}_{12} submatrices of the equations will be the FEM stiffness matrix with the rows corresponding to interface nodes removed. NEWROW now contains the coupled system equation numbers that correspond to each row in the finite element stiffness matrix.

With the NEWROW array complete the submatrices associated with the FEM can now be developed. The major effort involves reading the stiffness terms from the data file and inserting them into the coupled system. Because of the nonsymmetric coupling, each stiffness term is placed in two positions within the coupled system. In this implementation the two positions for the stiffness term are not, in general, symmetric either; this is due to the manner in which interface DOFs of the stiffness matrix are coupled for equilibrium.

In the PASBFI program the stiffness submatrices and [A] are developed in one algorithm and the known vector submatrix is developed later. The known vector submatrix is relatively simple to construct given the NEWROW array, so emphasis here is placed upon development of submatrices in the coefficient matrix. The algorithm is outlined as

```
initialize JCOL to PFEMCOL - 1
FOR each column of the FEM equations (J)
  increment the JCOL pointer by 1
  initialize the ICOL pointer to JCOL + 1
  IF the column number corresponds to an interface DOF
    (NEWROW[J] < PFEM)
      THEN put a -1 in the proper term of -[A] given by
        (A[NEWROW[J]-2*NUMINTEL,JCOL] = -1)
  skip the skyline pointer value (MAXA) in the STIFF file
  READ the number of terms in the Jth column (TOP)
  FOR each term in the column (I = J DOWNTO J-TOP+1)
    decrement the ICOL pointer by 1
    READ a term from STIFF into A[NEWROW[I],JCOL]
    IF this is not a diagonal term (I ≠ J)
      THEN place it in the NEWROW[J] row
        (A[NEWROW[J],ICOL] = a[NEWROW[I],JCOL])
  next term in the column
next column
```

After inserting the FEM load vector into the coupled vector of known values the system of equations can be solved. The artificial boundary loads and displacements are directly written to the output files. Then the response programs BEMIII and FEMIII calculate the internal responses for the boundary and finite element domains, respectively.

INSTRUCTIONS

The Naval Civil Engineering Laboratory has revised its primary distribution lists. The bottom of the mailing label has several numbers listed. These numbers correspond to numbers assigned to the list of Subject Categories. Numbers on the label corresponding to those on the list indicate the subject category and type of documents you are presently receiving. If you are satisfied, throw this card away (or file it for later reference).

If you want to change what you are presently receiving:

- Delete – mark off number on bottom of label.
- Add – circle number on list.
- Remove my name from all your lists – check box on list.
- Change my address – line out incorrect line and write in correction (ATTACH MAILING LABEL).
- Number of copies should be entered after the title of the subject categories you select.

Fold on line below and drop in the mail.

Note: Numbers on label but not listed on questionnaire are for NCEL use only, please ignore them.

Fold on line and staple.

DEPARTMENT OF THE NAVY

NAVAL CIVIL ENGINEERING LABORATORY
PORT HUENEME, CALIFORNIA 93043

OFFICIAL BUSINESS

PENALTY FOR PRIVATE USE, \$300
1 IND-NCEL-2700/4 (REV. 12-73)
0930-LL-L70-0044

POSTAGE AND FEES PAID
DEPARTMENT OF THE NAVY
DOD-316



Commanding Officer
Code L14
Naval Civil Engineering Laboratory
Port Hueneme, California 93043

DISTRIBUTION QUESTIONNAIRE

The Naval Civil Engineering Laboratory is revising its primary distribution lists.

SUBJECT CATEGORIES

1 SHORE FACILITIES

- 2 Construction methods and materials (including corrosion control, coatings)
- 3 Waterfront structures (maintenance/deterioration control)
- 4 Utilities (including power conditioning)
- 5 Explosives safety
- 6 Construction equipment and machinery
- 7 Fire prevention and control
- 8 Antenna technology
- 9 Structural analysis and design (including numerical and computer techniques)
- 10 Protective construction (including hardened shelters, shock and vibration studies)
- 11 Soil/rock mechanics
- 13 BEQ
- 14 Airfields and pavements
- 15 **ADVANCED BASE AND AMPHIBIOUS FACILITIES**
- 16 Base facilities (including shelters, power generation, water supplies)
- 17 Expedient roads/airfields/bridges
- 18 Amphibious operations (including breakwaters, wave forces)
- 19 Over-the-Beach operations (including containerization, materiel transfer, lighterage and cranes)
- 20 POL storage, transfer and distribution
- 24 **POLAR ENGINEERING**
- 24 Same as Advanced Base and Amphibious Facilities, except limited to cold-region environments

28 ENERGY/POWER GENERATION

- 29 Thermal conservation (thermal engineering of buildings, HVAC systems, energy loss measurement, power generation)
- 30 Controls and electrical conservation (electrical systems, energy monitoring and control systems)
- 31 Fuel flexibility (liquid fuels, coal utilization, energy from solid waste)
- 32 Alternate energy source (geothermal power, photovoltaic power systems, solar systems, wind systems, energy storage systems)
- 33 Site data and systems integration (energy resource data, energy consumption data, integrating energy systems)

34 ENVIRONMENTAL PROTECTION

- 35 Solid waste management
- 36 Hazardous/toxic materials management
- 37 Wastewater management and sanitary engineering
- 38 Oil pollution removal and recovery
- 39 Air pollution
- 40 Noise abatement
- 44 **OCEAN ENGINEERING**
- 45 Seafloor soils and foundations
- 46 Seafloor construction systems and operations (including diver and manipulator tools)
- 47 Undersea structures and materials
- 48 Anchors and moorings
- 49 Undersea power systems, electromechanical cables, and connectors
- 50 Pressure vessel facilities
- 51 Physical environment (including site surveying)
- 52 Ocean-based concrete structures
- 53 Hyperbaric chambers
- 54 Undersea cable dynamics

TYPES OF DOCUMENTS

85 Techdata Sheets

86 Technical Reports and Technical Notes

82 NCEL Guide & Updates

None—

83 Table of Contents & Index to TDS

91 Physical Security

remove my name

PLEASE HELP US PUT THE ZIP IN YOUR
MAIL! ADD YOUR FOUR NEW ZIP DIGITS
TO YOUR LABEL (OR FACSIMILE),
STAPLE INSIDE THIS SELF-MAILER, AND
RETURN TO US.

(fold here)

DEPARTMENT OF THE NAVY

NAVAL CIVIL ENGINEERING LABORATORY
PORT HUENEME, CALIFORNIA 93043-5003

OFFICIAL BUSINESS

PENALTY FOR PRIVATE USE, \$300

1 IND-NCEL-2700/4 (REV. 12-73)

0930-LL-L70-0044

POSTAGE AND FEES PAID
DEPARTMENT OF THE NAVY
DOD-316



Commanding Officer
Code L14
Naval Civil Engineering Laboratory
Port Hueneme, California 93043-5003